Referee 1
Interactive comment on "Drivers of the spatial phytoplankton gradient in estuarine-coastal systems: generic implications of a case study in a Dutch tidal bay" by Long Jiang et al.
Tom Fisher (Referee)
fisher@umces.edu
Received and published: 6 March 2020

This is a well-written, multi-disciplinary manuscript addressing the distribution of phytoplankton and primary productivity in a Dutch estuary. The three approaches (observational, modeling, remote sensing) provide a strong basis for describing phytoplankton distributions and the causes of the patterns. The literature synthesis at the end of the manuscript sets the results of this manuscript in global context. Overall, a strong addition to the estuarine literature.

Response (1): We appreciate the referee's efforts in reading our manuscript and positive comments. The manuscript has been revised based on the following suggestions.

I suggest that the authors address a few issues that I think are missing: 1. Light limitation of phytoplankton growth is common in estuaries and often occurs in turbid, nutrient-rich, low-salinity waters with no vertical stratification. No data are presented on salinity or density in this manuscript, and the authors simply state that there is no stratification, citing another paper. They could be right, and water depth may limit vertical mixing. However, my experience suggests that vertical stratification in spring under high river flow conditions initiates the spring bloom. Even if there are no CTD data available to calculate vertical variations in density, the authors should at least mention the possibility that the low salinity areas with high nutrients and turbidity may be light-limited regions of the estuary.

Response (2): Thanks for the comment. The Oosterschelde used to be a coastal plain estuary, but not any more since the safety-oriented Delta Works in the late 1980s (https://en.wikipedia.org/wiki/Delta_Works). Many dams and sluices were built at approximately the same time cutting the freshwater input of the Oosterschelde, which became isolated from other delta networks (Ysebaert et al., 2016). The overall freshwater inflow into the bay is below 10 m^3 s^{-1} (Ysebaert et al., 2016). For example, it was 3.2 m^3 s^{-1} and 4.5 m^3 s^{-1} in 2009 and 2010, respectively (Rijkswaterstaat data). This is a negligible amount compared to the flushing of the basin by tidal exchange, which is ~2 × 10^4 m^3 s^{-1}, estimated from a typical tidal prism of 9 × 10^8 m^3 in a 12-h tidal cycle.

Due to the greatly reduced freshwater input, the post-barrier Oosterschelde is well mixed most of the time. Based on our CTD casts in spring and summer, the surface-to-bottom salinity difference in a 10-m water column is below 0.1 psu (Figs.

R1 and R2).

Turbidity in the Oosterschelde does not resemble the typical distribution in an estuary. The suspended matter concentration is highest near the bay mouth and lowest near the northern branch where the aforementioned limited amount of freshwater enters (Wetsteyn and Kromkamp, 1994). In other words, the largest source of suspended sediment is the North Sea, rather than the landward end.

The Westerschelde, south to the Oosterschelde, is a true estuary with large freshwater and terrestrial of suspended sediment input, secchi depth of 0.2–2 m and salinity ranging 0 to 30. In contrast, the Oosterschelde is featured by greater transparency (secchi depth 3–5 m) and marine salinity conditions (salinity 30–33). Primary production in the Oosterschelde is much more limited by grazing and marine nutrient sources as discussed in the manuscript than light. Data in this paragraph are unpublished and measured by Jacco Kromkamp. We have clarified it in Section 2 (Page 3 Lines 23–25 in the "accept-changes" version) of the revised manuscript.
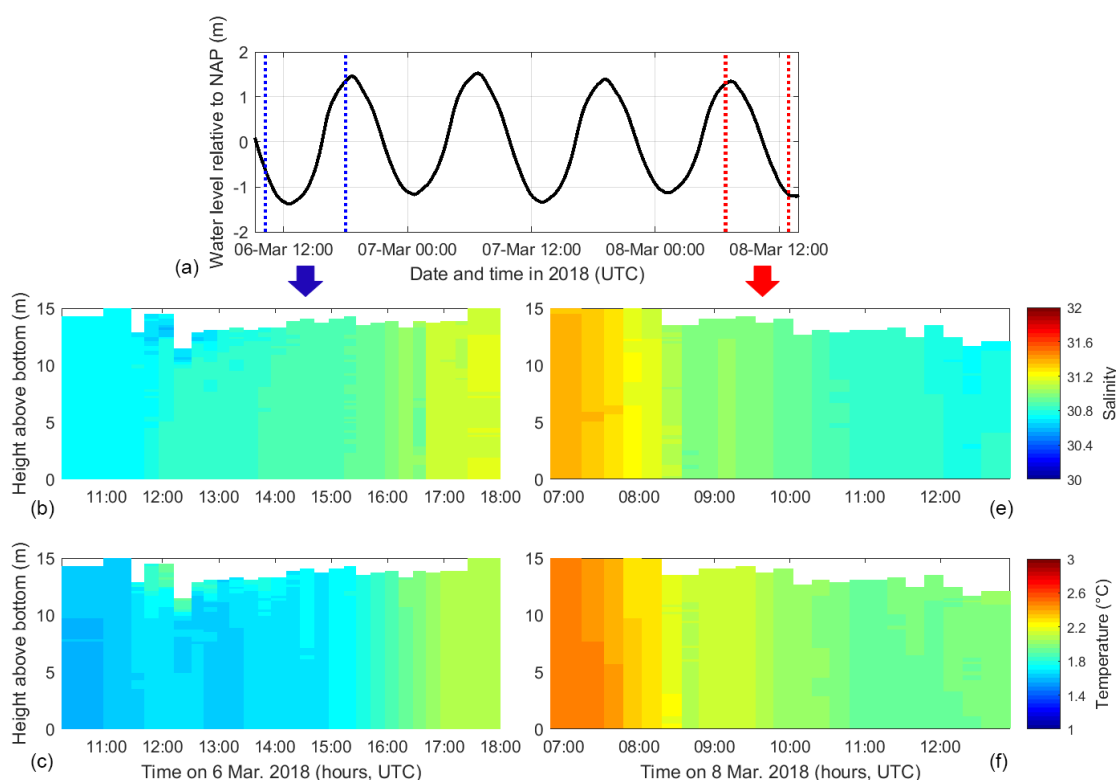
Figure R1: Observed (a) water level and (b-f) salinity and temperature at OS2. The station location is showed in Figure 2. The observational periods during flood (6 March 2018) and ebb (8 March 2018) tides are marked with blue and red dotted lines, and the corresponding observational data are shown in the lower left and right panels, respectively.
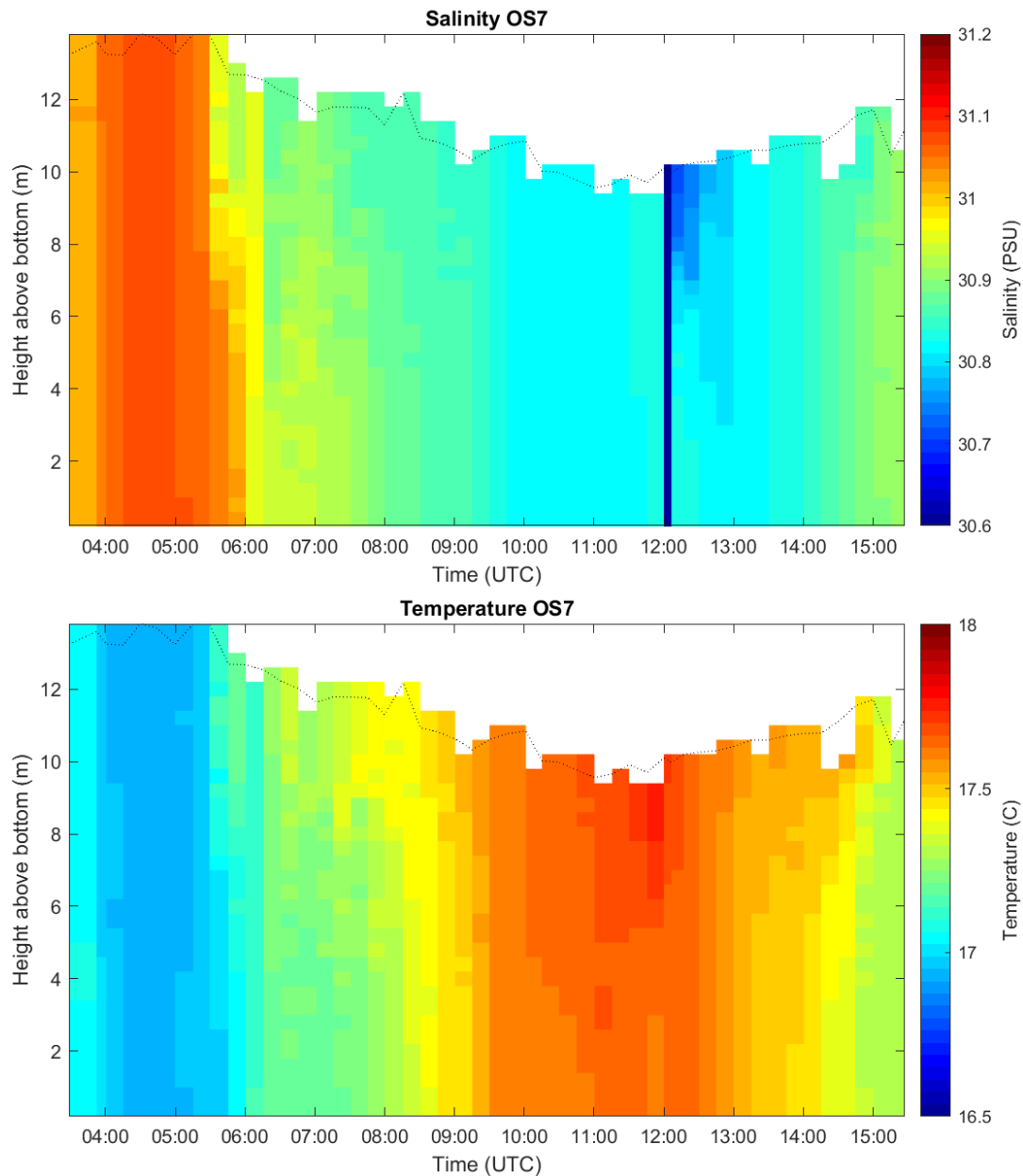
Figure R2: Observed salinity and temperature at OS7 during one full tidal cycle on 4 June 2019. The station location is showed in Figure 2. The water level is shown with the dotted line.

References

Wetsteyn, L. P. M. J., and Kromkamp, J. C.: Turbidity, nutrients and phytoplankton primary production in the Oosterschelde (The Netherlands) before, during and after a large-scale coastal engineering project (1980–1990), Hydrobiologia, 282/283, 61–78, http://doi.org/10.1007/BF00024622, 1994.

Ysebaert, T., van der Hoek, D. J., Wortelboer, R., Wijsman, J. W., Tangelder, M., and Nolte, A.: Management options for restoring estuarine dynamics and implications for ecosystems: A quantitative approach for the Southwest Delta in the Netherlands, Ocean Coast. Manage., 121, 33–48, https://doi.org/10.1016/j.ocecoaman.2015.11.005, 2016.

2. I am surprised that there are no data presented on salinity, temperature, river discharge, and river nutrient concentrations. The authors nicely show that advective inputs of shelf nutrients and phytoplankton is likely to be small, but never explore the role of river inputs. This could be a whole other paper, but they could at least mention that riverine inputs, both freshwater and nutrients, are likely driving the spring bloom. They could do additional model runs with half of the river discharge or half of the river N concentrations, but this might be more work than reasonable. I suspect that vertical stratification in the inner half of the estuary allows algal biomass to accumulate following high winter-spring river discharge. What would the model show if freshwater flow and/or river nutrient concentrations were halved? Can any of the temporal variations in the spring bloom be related to river flow?

Response (3): Thanks for the suggestion. The data on salinity, temperature, and river discharge is presented in the last response. The river nutrient is not significantly different from that in the Oosterschelde.

We conducted sensitivity test on the river discharge as suggested. A model run switching off the river discharge is compared with the baseline run. As we can see from the results (Figs. R3 and R4), dissolved inorganic nitrogen and chl-a are slightly higher in the baseline simulation including freshwater input, but the difference is minimal. The impact of freshwater is visible at OS5 but cannot reach the mainstem station OS2. These findings verify that freshwater input does not play a dominant part in the phytoplankton distribution in the Oosterschelde, as mentioned in the last response.

As readers may similarly wonder about the role of freshwater input, we have briefly added the above outlined explanation in Section 3.2 of the revised manuscript (Page 6 Lines 4–6 in the "accept-changes" version).
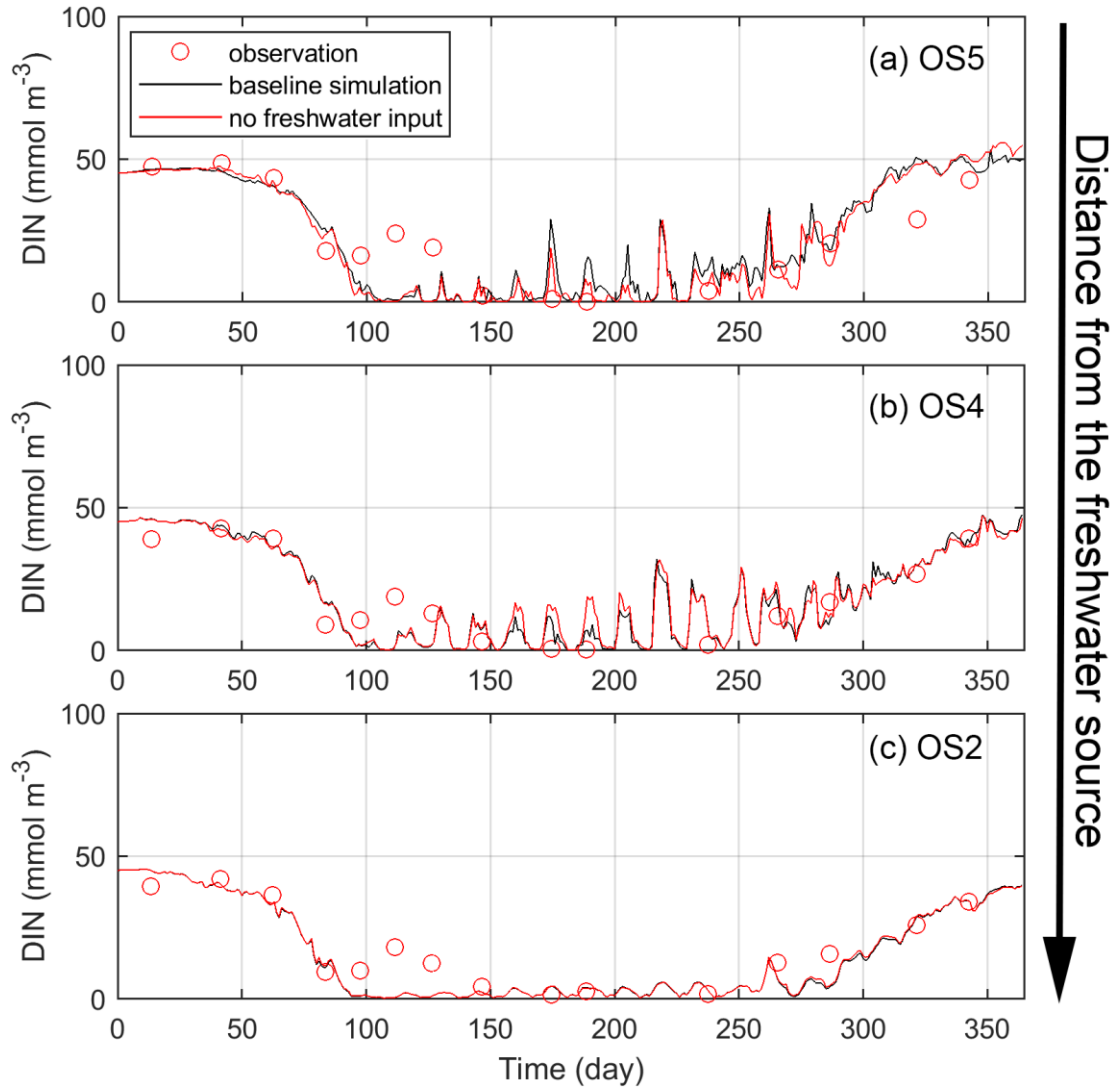
Figure R3: Comparison between modeled and observed dissolved inorganic nitrogen (DIN) in 2009 at stations(a) OS5, (b) OS4, and (c) OS2. The panels are arranged based on their respective distance from the freshwater source. See Figure 2 for station locations. The two model scenarios include the baseline scenario and switching off freshwater input.
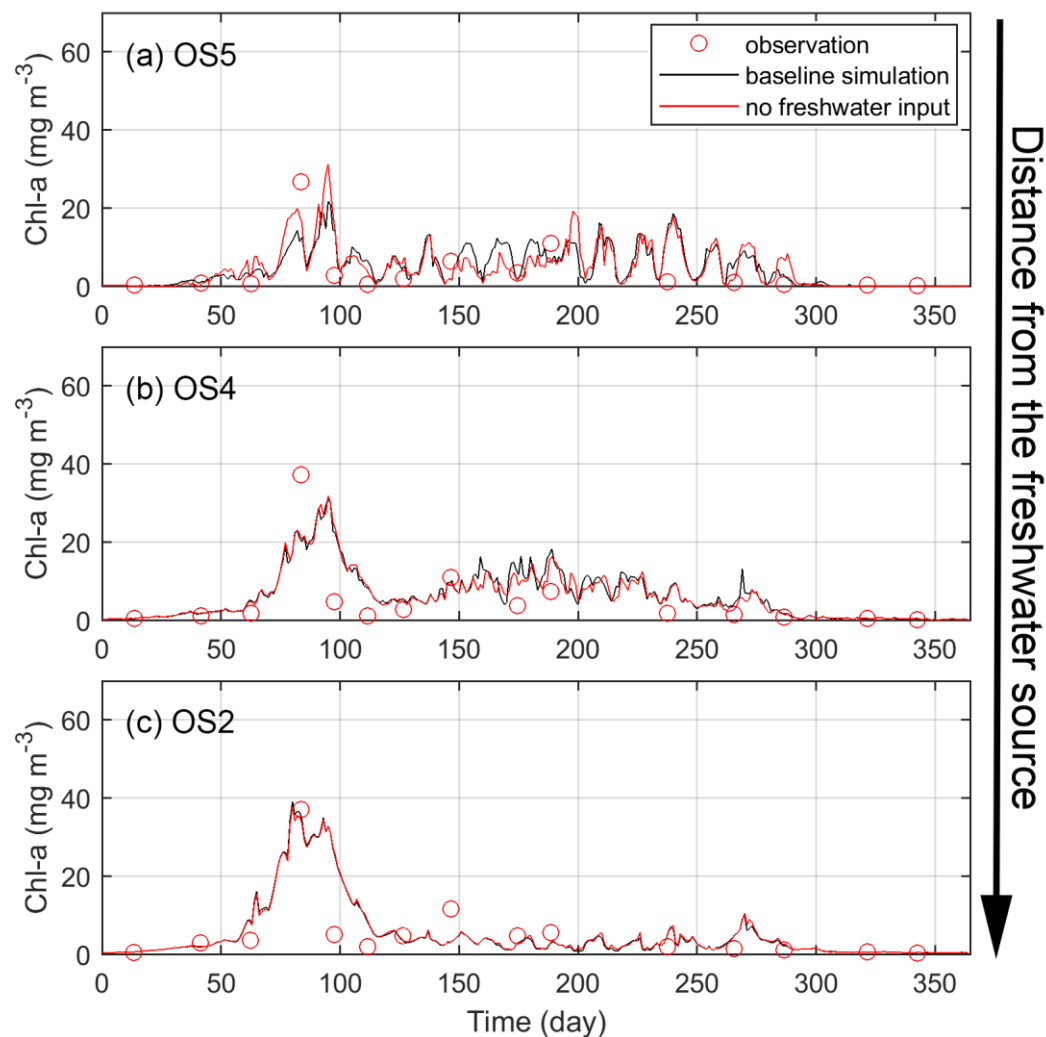
Figure R4: Comparison between modeled and observed chlorophyll-a in 2009 at stations (a) OS5, (b) OS4, and (c) OS2. The panels are arranged based on their respective distance from the freshwater source. See Figure 2 for station locations. The two model scenarios include the baseline scenario and switching off freshwater input.

3. I made a few minor grammatical or wording suggestions to the pdf of the text and for improvements in the figures that will be easy to address. This isn't a long manuscript, and the above two issues can probably be addressed briefly in 1-2 pages.

Please also note the supplement to this comment: https://www.biogeosciences-discuss.net/bg-2020-40/bg-2020-40-RC1-supplement.pdf

Response (4): The supplement is well received. Thanks for the minor suggestions, which are addressed as follows.

Page 4 Line 3-4: Not clearly stated. Bivalve grazing must also be burying and/or denitryfying phytoplankton N and P if grazing decreases prim prod. With no N and P losses, chla might decrease but primary production could be the same due to higher turnover.

Response (5): By grazing, bivalves remove N and P from the water column and keep the phytoplankton biomass low. On the other hand, bivalves release a smaller amount of inorganic nutrients into the water column by excretion and respiration, which may stimulate phytoplankton grown in the nutrient-limited summer months. We have removed the second half of the sentence for clarification. Please see Page 4 Line 9 in the "accept-changes" version of the revised manuscript.

Page 5 Line 10: validation? error rate or model accuracy? ok, I see it on p7. Add a sentence to Methods.

Response (6): We have changed it to "validation" and added this to the manuscript addressing the validation of the FABM model. Please see Page 5 Line 15 in the "accept-changes" version of the revised manuscript.

Page 5 Line 15: provide citation on sinking rate.

Response (7): We have added a reference (Eppley et al., 1967) here. Please see Page 5 Line 20 in the "accept-changes" version of the revised manuscript.

Reference
Eppley, R. W., Holmes, R. W., and Strickland, J. D. H.: Sinking rates of marine phytoplankton measured with a fluorometer, J. Exp. Mar. Biol. Ecol., 1, 191–208, https://doi.org/10.1016/0022-0981(67)90014-7, 1967.

Page 5 Line 26: specify weight ratio or give units. Also give a general range of PO4 concentrations to justify the N based model. Phytoplankton can be P and light-limited in the fresher parts of estuaries. Light limitation often occurs in the turbid 0-5 psu range, but no information seems to be available on vertical density and may not be available.

Response (8): Thanks for the comment. The unit of Chl:N ratio is mg Chl mmol N^{-1}, and the value (2) is prescribed based on the estimation of local species by Soetaert et al., 2001. Please see Page 5 Line 31 in the "accept-changes" version of the revised manuscript.

The PO_4 concentration ranges 0–2 mmol m^{-3} (Fig. R5). Most time of the year, phosphorus is not limiting, except for a short period after the spring bloom. We have mentioned it in the Discussion that not including P limitation may result in the underestimation of DIN in this period. Please see Page 9 Lines 6–10 in the

As described in Responses (2) and (3), the freshwater inflow is extremely low. The turbid fresh (0-5 PSU) region and strong vertical salinity gradients hardly exist in the Oosterschelde.
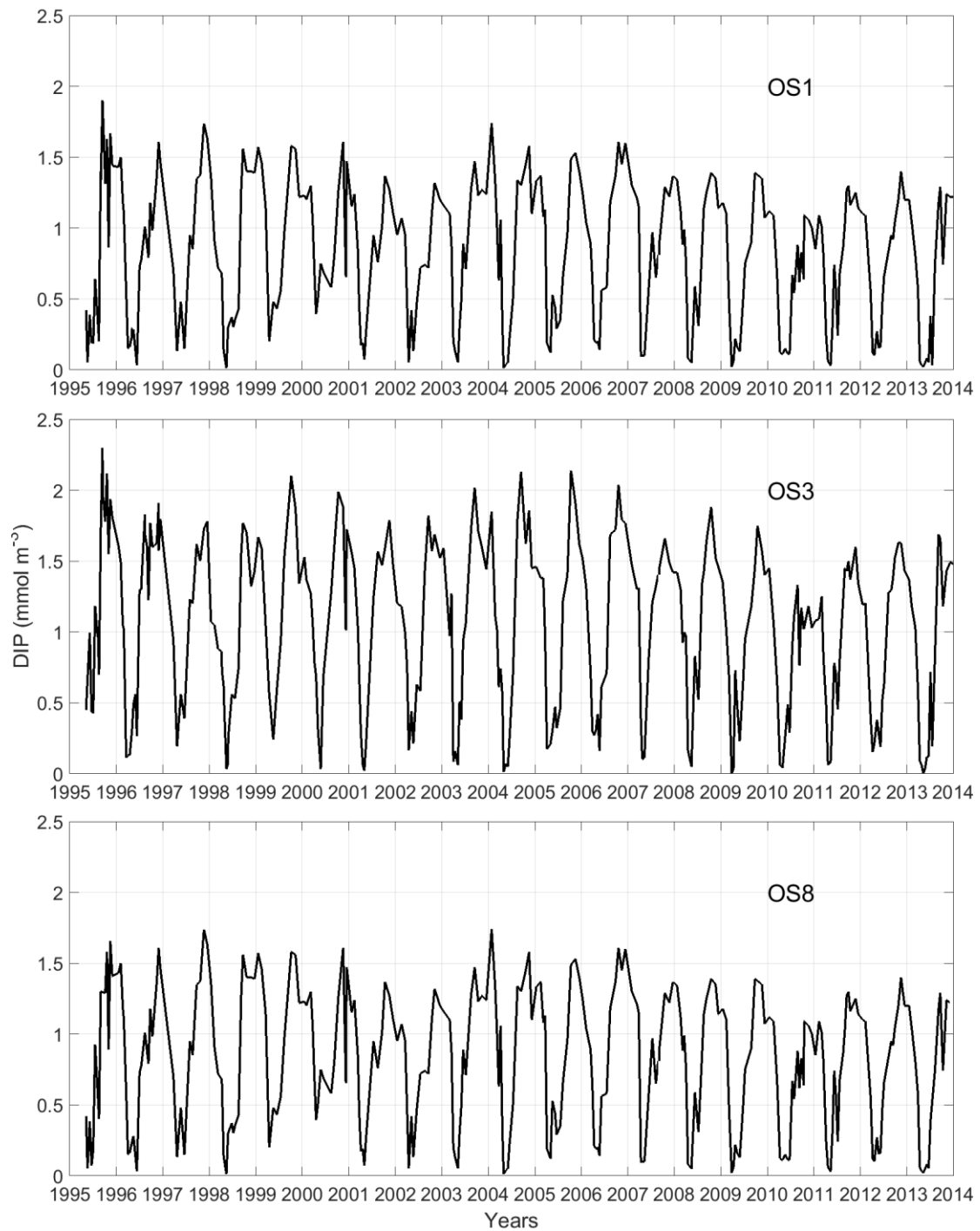
Figure R5: Time series of phosphate concentration during 1995–2013 at NIOZ stations OS1, OS3, and OS8.

Reference

Soetaert, K., Herman, P. M., Middelburg, J. J., Heip, C., Smith, C. L., Tett, P., and Wild-Allen, K.: Numerical modelling of the shelf break ecosystem: reproducing benthic and pelagic measurements, Deep-Sea Res. Pt. II, 48, 3141–3177, http://doi.org/10.1016/S0967-0645(01)00035-2, 2001.

Page 6 Line 21: winter phytoplankton blooms can occur in estuaries at low temperatures. Vertical stratification, sometimes defined by <0.5 psu, is the dominant control by limiting the depth of mixing in turbid waters especially with high FW flows.

Response (9): This comment also relates to our unclear description of the limited freshwater contribution. The Oosterschelde is not a typical estuary with high freshwater input. We have made the clarification here. Please see Page 6 Lines 26–27 in the "accept-changes" version of the revised manuscript.

Page 6 Lines 29-30: Was there any relationship between peak or integrated biomass and total river flow into the estuary? I'm guessing that the big or sustained peaks are positively associated with river discharge during the bloom period.

Response (10): Yes, the phytoplankton biomass at station RWS1 (at the mouth of the Westerschelde Estuary) is mostly influenced by the discharge of the Westerschelde. But for the most parts of the Oosterschelde, as presented in the manuscript, grazing pressure is the dominant control on phytoplankton biomass.

Page 8 Lines 22-25: Mention in methods that this issue is addressed in Discussion.

Response (11): OK. This relates to Response (8).

Page 8 Line 31: add a little more detail on how this was calculated here.

Response (12): Thanks for the suggestion. There are many ways to calculate residence time, and it is necessary to indicate the calculation here. The residence time is estimated by two methods in a model tracer experiment (Jiang et al., 2019). Briefly, each grid cell is filled with tracer and these two methods quantify the decay rate of tracer. The first method integrates the remnant function to calculate residence time

$T_r = \int_0^\infty C(t)/C_0 dt$, where $C(t)$ and C_0 are the instantaneous and initial tracer

concentration in each grid cell. The second method quantifies the time when $C(t) = e^{-1} C_0$, since the tracer concentration decreases exponentially in a well-mixed system. Based on our estimate, these two methods result in similar residence time in our system. We have added these two methods to the sentence. Please see Page 9 Lines 17–18 in the "accept-changes" version of the revised manuscript.

Reference

Jiang, L., Soetaert, K., and Gerkema, T.: Decomposing the intra-annual variability of flushing characteristics in a tidal bay along the North Sea, J. Sea Res., 101821, https://doi.org/10.1016/j.seares.2019.101821, 2019.

Page 9 Line 21: but nutrients are probably increasing towards the river end member due to light limitation of algal growth in the inner estuary.

Response (13): Because of the "missing" or weak river end member, the spatial gradients of nutrients and turbidity are not as strong as those in typical estuaries. Thereby, we differentiate the Oosterschelde, representing coastal bays with limited freshwater input but dominant marine influences, from river-dominated systems and other types in Section 6.

Page 9 Line 32: substantial land-derived nutrients, and light limitation of phytoplankton in turbid, low salinity areas of the estuary.

Response (14): This comment also relates to our unclear description of the limited freshwater contribution in the Oosterschelde. Because of that, the largest nutrient source is the marine import, contributing to the seaward increasing chl-a distribution.

Page 10 Line 10: is maintained

Response (15): Corrected. Please see Page 11 Line 9 in the "accept-changes" version of the revised manuscript.

Page 11 Line 26: trophic levels.

Response (16): Thanks for the correction. This sentence is rephrased. Please see Page 12 Line 27 in the "accept-changes" version of the revised manuscript.

Page 11 Line 28: This is barely addressed. Either add likely climate effects to Discussion or remove this statement here and in Abstract.

Response (17): Thanks for the suggestion. The climate effect is deleted here and in Abstract. Please see Page 12 Lines 22–28 and Page 1 Lines 24–25 in the "accept-changes" version of the revised manuscript.

Figure 5: The time axis of Figs 4 and 5 is not sufficiently clear to tell when the blooms occur. They said it was spring, but it would be easy to add month or half-year tics to show this more clearly.

Response (18): Thanks for the suggestion. We have changed the interval of grid lines to two months in Fig. 4, and Fig. 5 has been replaced with a monthly average graph.

Referee 2
Interactive comment on "Drivers of the spatial phytoplankton gradient in estuarine-coastal systems: generic implications of a case study in a Dutch tidal bay" by Long Jiang et al.
Nicole Millette (Referee)
nmillette@vims.edu
Received and published: 11 March 2020

This is one of the most well-written papers I have reviewed and everything was well laid out and easy to follow. However, I was left with wanting a lot more information and discussion from the authors. This is the first time I have ever said this, but this paper is too short. There are three different approaches used in the paper, which is a plus, but there is a lot of information that could be shared about each approach. The main conclusions for the paper are clear and well supported, but this is a case study, and I think there should be a lot more acknowledgement and discussion of the nuances in the variability of the spring bloom in the Oosterschelde; it has not always followed the described pattern. More specifics are provided below:

Response: The referee's constructive suggestions are much appreciated. We have revised the manuscript and provided the suggested information. Please see the following point-by-point replies.

General Comments
1. More information and discussion of the field data
(a) Page 6, line 17-20: There is some discussion in here about how nutrients, light, and temperature effect the phytoplankton biomass annual cycle, but none of the data presented demonstrate or support these claims. What is this based off of, other people's findings or the authors own analysis? If these are the authors own conclusions, then I would like to see data and analysis to support these claims.

Response (G1a): Thanks for the comment. We have added the model results of temperature, nutrients, and light factors affecting the growth rate (Fig. 8) and explained the seasonal controls of phytoplankton variability in Section 4.2 (Page 7 Lines 19–29 in the "accept-changes" version of the revised manuscript). In winter, the low chl-a is a result of low temperature and light conditions that improve in March and April and initiates the spring bloom. The bloom algae consume nutrients and lead to post-bloom nutrient limitation. In late summer and early fall, light, nutrients, temperature still fuel high growth rate, while the low biomass results from grazing. When temperature and light start constraining primary production, the chl-a decreases and nutrients accumulates, entering the next annual cycle.

(b) A figure of DIN concentrations, similar to figure 4, would be beneficial.

Response (G1b): Thanks for the suggestion. We have plotted the 19-yr timeseries of

11

DIN. DIN at the offshore station RWS2 is consistently lower than RWS1 and other inner-bay stations, while the stations inside the Oosterschelde show little difference in DIN concentration from each other (Fig. R1). Thus, the DIN spatial heterogeneity in the bay is not as strong as chl-a (Fig. 4). Given that the DIN annual cycle is presented in Fig. 6, Fig. R1 is not included in the manuscript.
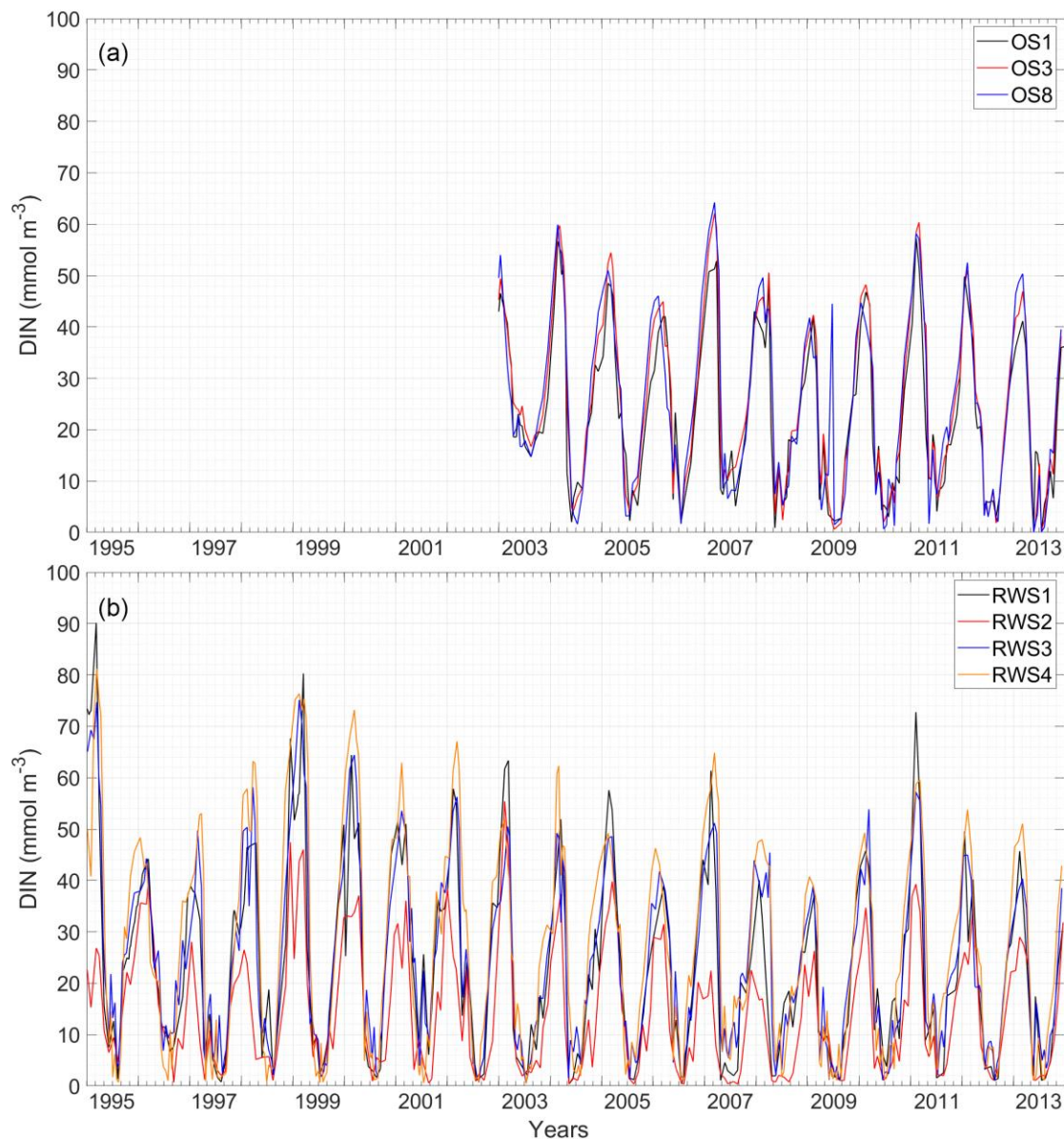
Figure R1: Time series of DIN (dissolved inorganic nitrogen) concentration during 1995–2013 at (a) NIOZ stations OS1, OS3, and OS8 and (b) Rijkswaterstaat stations RWS1–RWS4. Intervals between grid lines indicate two months. See Figure 2 for station locations.

(c) Why is OS6 not included in figure 2?

Response (G1c): OS6 is to the north of OS5 and not in the model domain. Thus, OS6 is not presented in the map.

(d) Page 4, line 16-17: More information on the 14CO2 uptake experiments would be helpful - Who did the experiments? At all stations? For all sample dates in 2010? Is this data published elsewhere?

Response (G1d): One of our co-authors Jacco Kromkamp did the experiments. The measurements were done at stations OS2 and OS8, as shown in Fig. 7, and yes, for all sample dates in 2010. The data is not published before. We have added the suggested information to Section 3.1 and Author contributions. Please see Page 4 Lines 21–22 and Page 13 Lines 8–9 in the "accept-changes" version of the revised manuscript.

(e) The SD bars in figure 2 are large for both gradients, suggesting a wide range of [chla] at all stations during spring between 1995 and 2013. The average values show a tendency towards higher [chla] at the mouth, but the large SD demonstrate a lot of inter-annual variability. Based on figure 4a, it appears that the pattern in spring phytoplankton biomass described in this paper dominated between 2000 and 2009. Pre-2000, [chla] at the head and mid-bay repeatedly matched or surpassed the mouth, 1998 being the clear exception. After 2009, [chla] during spring appears to become less distinct between each location. This does not negate the conclusions of the paper, but the years that do not match the pattern should be acknowledged. It is not expected that every year will always be the same, so what might have happened in the years that didn't follow the pattern?

Response (G1e): Good point. We agree with the referee that the spatial chl-a gradient shown in Fig. 2 is not universal in every year in Fig. 4. The gradient is obvious overall (Fig. 5), especially in some years (such as in 2005 and 2008 in Fig. 4a) and not so much in other years (such as in 1997 and 2012 in Fig. 4a). There are several potential causes.

Firstly, due to shallowness and being surrounded by land, water in the bay head is heated up slightly faster than that in the North Sea, so the spring bloom sometimes occurs several days earlier. If the sampling activity happens during the bloom in the North Sea, the chl-a distribution shows a seaward increasing trend. However, if the measurement is undertaken during the bloom in the bay, the bay head may exhibit higher phytoplankton biomass. For example, the peak biomass at the seaward end occurred later than at the landward end in Years 1996, 1997, and 2005 (Fig. 4b), whereas the spring bloom of the entire basin happens almost at the same time in Years 2002 and 2008 (Figs. 4a and 4b). Moreover, the chl-a concentration tends to be slightly higher in the landward end in February (Fig. 5). Thus, the interannual variability of the spring bloom timing can contribute to changes in the spatial chl-a gradient.

Secondly, the sampling frequency is usually biweekly or even monthly, so one data point in the time series may miss the peak bloom or result in different spatial chl-a

distribution. For instance, in 2010, the overall magnitude of the spring bloom is relatively low, and the spatial chl-a gradient is more obvious in the RWS data than in the NIOZ data due to different sampling dates (Figs. 5a and 5b).

Given the above concerns, the seaward increasing chl-a gradient may not be discernible in one year's data. Therefore, we present the gradient with the average biomass in March to May during 19 years (Fig. 2), as well as by month (Fig. 5). The large standard deviations in Figs. 2 and 5 do include the interannual variability as the referee suggests. Note that the phytoplankton biomass before, during, and after the spring bloom also creates large variability in three months, which is another source of the presented standard deviations. We have added a paragraph in Discussion including these effects of temporal variability on the spatial phytoplankton distribution. Please see Page 10 Lines 3–13 in the "accept-changes" version of the revised manuscript.

2. More information and discussion of the model results (a) Figure 6, 7, 9: Are the field observations in these figures averages? If there is any way to calculate the standard deviation for these values, it should be included.

Response (G2a): The mesotidal Oosterschelde is well-mixed vertically (see the CTD casts of temperature and salinity at OS7 in Fig. R2 for example). For DIN and chl-a observations shown in Figs. 6 and 9 (now Fig. 10), the NIOZ and Rijkswaterstaat monitoring programs use the near-surface sample to represent the entire water column. Thus, unfortunately, there is no three measurements or replicates at each station to calculate the standard deviations.

For the *NPP* data in Fig. 8 (now Fig. 9), light attenuation was measured once during the cruise and the overall primary production is an integration of the entire water column. That is, we have only one *NPP* result for each station on each sampling date and are unable to calculate the standard deviations for *NPP*.
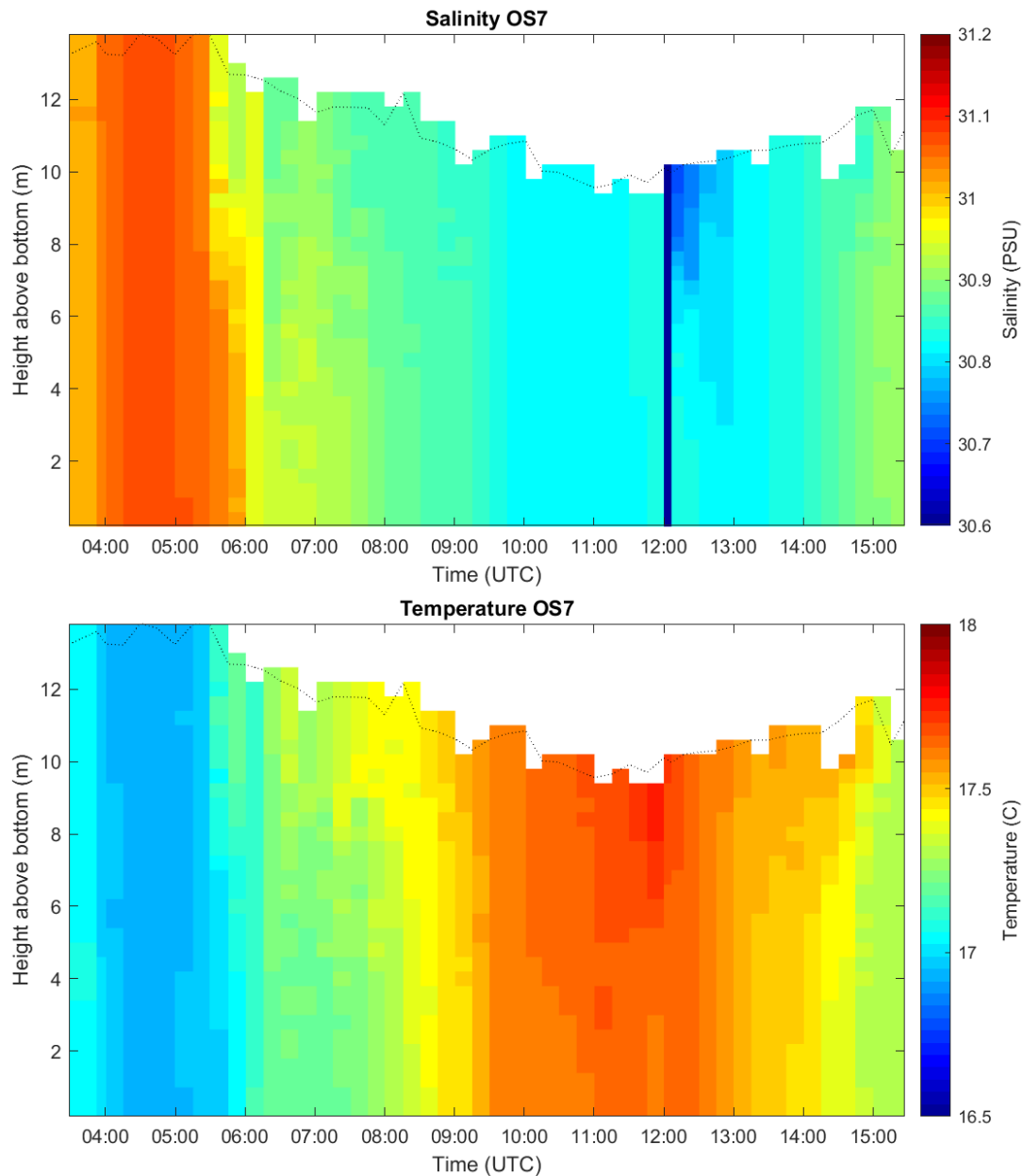
Figure R2: Observed salinity and temperature at OS7 during one full tidal cycle on 4 June 2019. The station location is showed in Figure 2. The water level is shown with the dotted line.

(b) Page 7, line 12: The authors mention that before the bloom, phytoplankton biomass and growth rates were low, but this data is not really presented. I know [chla] = phytoplankton biomass, so maybe keep the terminology consistent in the paper. However, the growth rate data from the model is something that I think should be presented, it sounds like it is interesting.

Response (G2b): Thanks for the comment. Primary production is the product of phytoplankton biomass and growth rate. In our model formulation, growth rate is a function of temperature, nutrient, and light factors, as shown in Equation (2) in Table 1. We have extracted these three factors from the model (Fig. 8). Their product should

15

be proportional to the growth rate and be used to denote the relative changes in the growth rate (Fig. 8). The discussion based on biomass and growth rate has been updated with the new figure included. Please see Page 7 Lines 19–29 in the "accept-changes" version of the revised manuscript.

(c) Page 7, line 17-18: I wanted more detail here, rather than saying NPP is generally higher at OS8 compared to OS2. The authors note that the model overestimates NPP at OS8 in the fall 2010, but that overestimation makes it difficult to compare the two sites in figure 7. What is the average + SD observed NPP at each station? Is it significantly different? On average, how much higher is NPP at OS8 compared to OS2 in observed and modeled data?

Response (G2c): Thanks for the suggestion. The observed *NPP* at OS8 and OS2 is 902.6 ± 928.4 mmol C m^{-2} d^{-1} and 722.5 ± 794.6 mmol C m^{-2} d^{-1}, respectively. Although the observed NPP at OS8 is slightly higher, their difference is not significant according to the t-test ($t = 0.59$, $p > 0.05$, $n = 16$). In contrast, the modeled *NPP* at OS8 (1033.9 ± 1084.3 mmol C m^{-2} d^{-1}) is significantly higher that OS2 (606.0 ± 499.5 mmol C m^{-2} d^{-1}) according to the t-test ($t = 6.85$, $p < 0.05$, $n = 365$). We have added these statistical analyses to the revised manuscript. Please see from Page 7 Line 29 to Page 10 Line 2 in the "accept-changes" version of the revised manuscript.

(d) Figure 7: The authors explain the overestimation at OS8, but why did the model miss the highest peak in NPP at both stations around day 175?

Response (G2d): Good question. The modeled *NPP* is influenced by temperature, nutrients, light, and phytoplankton biomass. Light and temperature is reasonably simulated by the hydrodynamic model (Jiang et al., 2019), and the slight deviation of simulated chl-a (Day 540 in Fig. 6) cannot fully explain the underestimation of *NPP*, which, thus, is related to nutrients. Fig. 7 show that the underestimation of *NPP* actually starts right after the spring bloom (Day 125) and lasts till around Day 175. This is a period that DIN is underestimated (Days 490–540 in Fig. 6). As discussed in the manuscript, this results from our N-based model excluding the effect of phosphorus or silicon limitation. Therefore, DIN is depleted too early and thus limiting *NPP* (Fig. 8), which should decline more slowly or even increase slightly (Fig. 7). We have added these discussions in Sections 4.2 and 5. Please see Page 7 Line 27 and Page 9 Lines 6–10 in the "accept-changes" version of the revised manuscript.

Reference

Jiang, L., Gerkema, T., Wijsman, J. W., and Soetaert, K.: Comparing physical and biological impacts on seston renewal in a tidal bay with extensive shellfish culture, J. Mar. Syst., 194, 102–110, http://doi.org/10.1016/j.jmarsys.2019.03.003, 2019.

3. My personal opinion is the synthesis section (6) does not belong in this paper. Figure 12 and all the work the authors did is very interesting, but does not fit with the rest of the paper. Figure 12 and the synthesis sections should be its own paper. There is a lot of information in figure 12 that deserves more than three paragraphs of explanation. A case study of chlorophyll a spatial pattern in the Oosterschelde is not the place to propose a categorization of chlorophyll a spatial patterns for all estuaries.

Response (G3): Thanks for the comment. Section 6 is originally part of Discussion and aims to put the Oosterschelde in broader context of global estuaries and coastal bays. In comparing the different spatial phytoplankton distribution patterns, main drivers of the phytoplankton gradient are discussed. The general lesson from this section is that the spatial phytoplankton distribution is usually shaped by one or more environmental drivers that differ from system to system. This is the basis of the "general implication" in the title. Therefore, we consider this part important in terms of extending the discussion on key environmental controls of phytoplankton distribution and gaining the interest to a broad audience and tend to retain it. Two other referees are also in support of this section.

Specific Comments
1. Introduction Page 2, line 28 – Page 3, line 1: Include the pros and cons of all three methods. No cons are mentioned for ecological methods.

Response (S1): If we understand this correctly, the referee suggests us to describe the cons of numerical ecological models, not ecological methods. The drawbacks or limitations of numerical models are they are based on simplified assumptions and cannot simulate every detail in nature. Thus, a useful or reliable model has to be calibrated and validated by observed or measured in situ data. We have added the above information to the paragraph. Please see from Page 2 Line 34 to Page 3 Line 1 in the "accept-changes" version of the revised manuscript.

2. Methods Page 5, line 24-26: The model output results went through two conversions to match the observation data (N->C, then C->chla). There should be some mention of the assumptions and limitations of these conversions because they are not perfect and there has recently been growing criticism of the C:chla ratio.

Response (S2): Thank you for the suggestion. Our text may be a bit confusing here. The model is nitrogen-based. Two conversions were involved. (1) The Redfield C:N ratio was used to convert the nitrogen-based modeled NPP to the carbon-based measured NPP as shown in Fig. 7. (2) The Chl:N ratio (Soetaert et al., 2001) was used to convert the modeled nitrogen-based phytoplankton biomass to the chl-a concentration. So the C:Chl-a ratio was not applied here. It is true that these ratios are variable in nature and our simplification in the model is not without limitations. We have also claimed the limitation in the first paragraph of Discussion. Please see Page

9 Lines 11–13 in the "accept-changes" version of the revised manuscript.

Reference

Soetaert, K., Herman, P. M., Middelburg, J. J., Heip, C., Smith, C. L., Tett, P., and Wild-Allen, K.: Numerical modelling of the shelf break ecosystem: reproducing benthic and pelagic measurements, Deep-Sea Res. Pt. II, 48, 3141–3177, http://doi.org/10.1016/S0967-0645(01)00035-2, 2001.

7. Summary Page 11, line 24-28: These last two sentences do not accurately sum up the paper. There is no discussion of temporal variability in the spatial distribution of phytoplankton in Oosterschelde and I did not get an understanding of phytoplankton's role as an ecological indicator. The paper would be greatly strengthened by a discussion of the temporal variability and what caused it.

Response (S3): Thanks for the comment. We agree that the manuscript focuses on the spatial pattern, which cannot be discussed without temporal variations. These two sentences have been rephrased to emphasize the temporal changes and natural and anthropogenic controls on phytoplankton distribution. Please see Page 12 Lines 22–28 in the "accept-changes" version of the revised manuscript.

Referee 3
Interactive comment on "Drivers of the spatial phytoplankton gradient in estuarine-coastal systems: generic implications of a case study in a Dutch tidal bay" by Long Jiang et al.
J. Blake Clark (Referee)
blake.clark@nasa.gov
Received and published: 7 April 2020

General Comments
This paper describes a coupled observational, modeling and satellite observational study of an estuarine system in the North Sea. Overall, the story and results were well conveyed and the conclusions regarding drivers of spatial and temporal variability in the estuary were supported. The main take away is that there is a Type I phytoplankton distribution and it is mainly driven by benthic grazing pressure in the landward stations. The model supports the importance of grazing pressure on the spatial distribution by numerically removing bivalves in the modeling system. Modeling estuarine primary production and chl-a distribution can be particularly challenging, and I think the author's did a pretty good job at capturing overall NPP magnitude and some of the temporal variability, compared to 14-C NPP incubation data. The synthesis at the end is particularly useful, especially related to the discussion of how different mechanisms can lead to similar patterns of chl-a distribution, depending on the system.

Response (1): Thanks for the positive feedback and the following suggestions. We have revised the manuscript as suggested and replied to the comments point by point.

The main methodology and results that need to be improved upon, or omitted, relates to the use of the satellite observations. The author's use one image (Fig. 10) and it doesn't really track with the results and conclusions of the rest of the paper. In fact, the chl-a concentration is highest in the landward stations where in most observations showed lower chl-a concentration. I understand the desire to do this coupled methodological approach, but in my opinion if satellite data is to be used, it should be developed a bit more to support the observational and modeling work. There is definitely a lot of value in using these data, but acquiring more spring bloom images from MERIS data that fall within the observational window would offer a bit more support for the other results.

Response (2): Thank you for the suggestions.

The Envisat MERIS satellite data can be used to retrieve chl-a concentrations at a spatial concentration of ca 300 m (FR, full resolution data) to ca 1 km (RR, reduced resolution data). Their spatial resolutions are typically not sufficiently high for the application of the Oosterschelde, because the narrowest portions of the basin and the northern branch are around 3 km , and the Oosterschelde has intertidal flats that fall

19

dry during low water (Fig. R1). Therefore, the land or intertidal pixels may interfere with the MERIS data in the Oosterschelde region.

van der Woerd et al. (2011) have investigated the surface chl-a in the North Sea with MERIS reduced resolution output. Their processed MERIS satellite data show that results within the Oosterschelde should be treated with caution, especially at narrow regions (Fig. R2). In contrast, the 10-m-resolution Sentinel-2 MSI data applied in our study have a spatial resolution suitable for the Oosterschelde.

In addition to the demand of a high spatial resolution, the satellite data to be used in our study also needs to be taken at high tides. One third area of the Oosterschelde is covered by intertidal flats and the water around the flats is extremely shallow (Nienhuis and Smaal, 1994). Bottom reflectance may become another source of errors at low tides (cf Arabi et al., 2019, for optically shallow water effects from MERIS full resolution images of the Wadden Sea). Availability of high tide, low cloud cover images that can show the overall spatial chl-a gradient in the Oosterschelde. are hence very limited.

Moreover, the satellite image in Fig. 11a offers, as a snapshot, valuable insight into the spatial gradient. The spatial phytoplankton pattern shown in Fig. 11a was also detected in the model output (Fig. 11b), which partly validates the model. Although the seaward increasing chl-a gradient is most common in the Oosterschelde in spring, it changes with time. That is, when discussing the spatial phytoplankton variability, we have to be aware of the temporal variability. When describing the general spatial gradient, the less general "exceptions" needs to be noticed. In the revised manuscript, we have emphasized the importance of temporal variability. The satellite image and the less frequent spatial gradient it displays (Fig. 11) fits in that standpoint. Thereby, we tend to retain Section 4.3 and Fig. 11a.
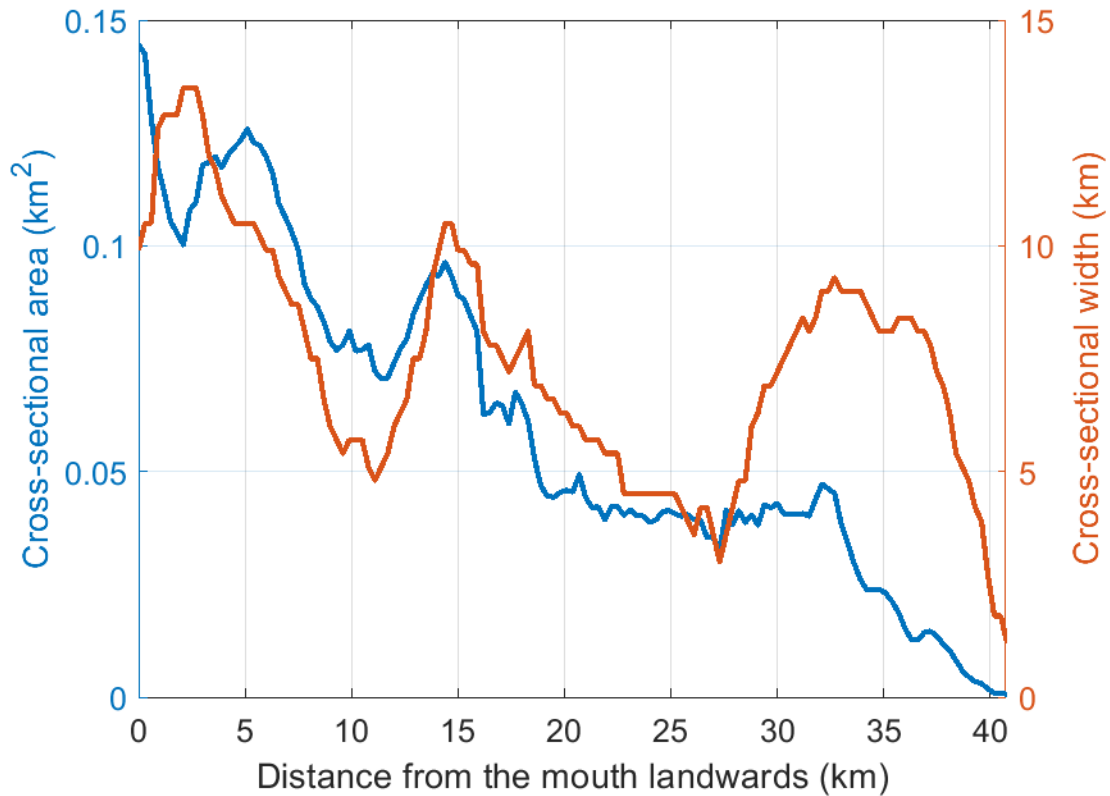
Figure R1: The cross-sectional area and width of the Oosterschelde from the mouth to its eastern end. The northern branch (Fig. 1) is excluded from the calculation because of a different orientation of channels. This figure is Fig. 6 in Jiang et al., 2020.

References

Arabi, B. , Salama, M. S. , Van der Wal, D., Pitarch, J. , and Verhoef, W.: The impact of sea bottom effects on the retrieval of water constituent concentrations from MERIS and OLCI images in shallow tidal waters supported by radiative transfer modeling, Remote Sens. Environ., 237, 11596, https://doi.org/10.1016/j.rse.2019.111596, 2020.

Jiang, L., Gerkema, T., Idier, D., Slangen, A. B. A., and Soetaert, K. E.: Effects of sea-level rise on tides and sediment dynamics in a Dutch tidal bay, Ocean Sci., 16, 307–321, https://doi.org/10.5194/os-16-307-2020, 2020.

Nienhuis, P. H., and Smaal, A. C.: The Oosterschelde estuary, a case-study of a changing ecosystem: an introduction, Hydrobiologia, 282/283, 1–14, http://doi.org/10.1007/BF00024616, 1994.

van der Woerd, H. J., Blauw, A., Peperzak, L., Pasterkamp, R., and Peters, S.: Analysis of the spatial evolution of the 2003 algal bloom in the Voordelta (North Sea), J. Sea Res., 65, 195–204, ttp://doi.org/10.1016/j.seares.2010.09.007, 2011.

Specific Comments

Page 2 Line 10: This sentence with the semi-colons is oddly structured, consider revising because the information is good.

Response (3): This sentence is rephrased and split into three sentences. Please see Page 2 Lines 10–13 in the "accept-changes" version of the revised manuscript.

4-20: "Light attenuation was measured : : :" How specifically was light attenuation measured and with what instrument?

Response (4): The light intensity (I, μmol photons m^{-2} s^{-1}) in underwater layers was measured in the field with Licor LI-192SB cosine-corrected light sensors connected to a Licor LI-185B quantum meter. Then the light extinction coefficient K_d and light distribution in the entire water column were calculated based on the Lambert-Beer Law, $I_z = I_0 * exp(-z*K_d)$, where I_0 and I_z are the light intensity at surface and depth z. We have added the information in the manuscript. Please see Page 4 Lines 25–27 in the "accept-changes" version of the revised manuscript.

4-25: "We used the measured values : : :" I don't quite understand this sentence, consider revising.

Response (5): "the measured values" have been changed to "the measured primary production data". Please see Page 4 Line 32 in the "accept-changes" version of the revised manuscript.

5-510: What weather forcing was used, specifically, and how was surface irradiance specified?

Response (6): We used atmospheric forcing including surface irradiance calculated from a downscaled weather model HARMONIE with a horizontal resolution of 2.5 km produced by the Royal Dutch Meteorological Institute (KNMI).

5-15: I see in the equations, detritus sinking is also calculated, but perhaps mention that here as well.

Response (7): Thanks for the suggestion. The sinking of detritus is added here. Please see Page 5 Lines 18–20 in the "accept-changes" version of the revised manuscript.

5-30: From what I can tell the bivalve biomass is constant, but perhaps clarify that here. Are the bivalves growing and dying or are they constant in time?

Response (8): Bivalves are growing and excreting nitrogen following the governing equation (22) in Table 1. However, our model does not account for the shellfish harvest mortality, occurring mostly in late summer. We have considered it as one of

22

the limitations of the model and discussed it in the first paragraph of Discussion. Please see Page 9 Lines 10–11 in the "accept-changes" version of the revised manuscript.

6-20:25: It would be useful to show some kind of climatology of the measurements with a window or errorbars that show the inter-annual variability. See figs in Testa, J. M., Murphy, R. R., & Brady, D. C. (2018). Nutrient-and climate-induced shifts in the phenology of linked biogeochemical cycles in a temperate estuary. Frontiers in Marine. https://www.frontiersin.org/articles/10.3389/fmars.2018.00114

Response (9): Thanks for the suggestion. We have replaced Fig. 5 with a climatology graph and updated the text accordingly.

9-20: Does the decreasing depth (presumably) also cause the benthic-pelagic coupling to become stronger? Are there bivalves in the more seaward stations but because there is a greater volume of water the grazing pressure just is less, on an areal basis?

Response (10): Good point. Yes, indeed. In a recent study about the spatial variability of tides in the Oosterschelde (Jiang et al., 2020), we found that the average depth and cross-sectional area decreases landwards (Fig. R1). This geometric feature induces tidal convergence, i.e., larger tidal amplitude at the landward end. Therefore, shallower water depth and stronger tidal mixing can contribute to stronger benthic pelagic coupling and higher benthic grazing pressure in the east of the basin. We have added this point here and in Discussion. Please see Page 9 Lines 17–20 and Page 10 Lines 16–17 in the "accept-changes" version of the revised manuscript.

Reference
Jiang, L., Gerkema, T., Idier, D., Slangen, A. B. A., and Soetaert, K. E.: Effects of sea-level rise on tides and sediment dynamics in a Dutch tidal bay, Ocean Sci., 16, 307–321, https://doi.org/10.5194/os-16-307-2020, 2020.

Drivers of the spatial phytoplankton gradient in estuarine-coastal systems: generic implications of a case study in a Dutch tidal bay

Long Jiang[1,2,3], Theo Gerkema[3], Jacco C. Kromkamp[3], Daphne van der Wal[3,4], Pedro Manuel Carrasco De La Cruz[5], and Karline Soetaert[3]

[1] Key Laboratory of Marine Hazards Forecasting, Ministry of Natural Resources, Hohai University, Nanjing, China
[2] College of Oceanography, Hohai University, Nanjing, China
[3] NIOZ Royal Netherlands Institute for Sea Research, Department of Estuarine and Delta Systems, and Utrecht University, P.O. Box 140, 4400 AC Yerseke, The Netherlands.
[4] Faculty of Geo-Information Science and Earth Observation (ITC), University of Twente, P.O. Box 217, 7500 AE, Enschede, Netherlands.
[5] NF-POGO Centre of Excellence, Alfred Wegener Institute, Kurpromenade 201, 27498 Helgoland, Germany.

Correspondence to: Long Jiang (ljiang@hhu.edu.cn)

Abstract. As the primary energy and carbon source in aquatic food webs, phytoplankton generally display spatial heterogeneity due to the complicated biotic and abiotic controls, but our understanding of its causes is challenging as it involves multiple regulatory mechanisms. We applied a combination of field observation, numerical modeling, and remote sensing to display and interpret the spatial gradient of phytoplankton biomass in a Dutch tidal bay (the Oosterschelde) on the east coast of the North Sea. The 19-year (1995–2013) monitoring data reveal a seaward increasing trend in chlorophyll a concentrations during the spring bloom. Using a calibrated and validated three-dimensional hydrodynamic-biogeochemical model, two idealized model scenarios were run, switching off the suspension feeders and halving the open-boundary nutrient and phytoplankton loading. Results indicate that bivalve grazing exerts a dominant control on phytoplankton in the bay and that the tidal import mainly influences algal biomass near the mouth. Satellite data substantiate the roles of benthic grazing and tidal import. Based on a literature review, the spatial phytoplankton gradients in global estuarine-coastal ecosystems are ~~classified into~~ summarized in five common types: seawards increasing, seawards decreasing, concave with a chlorophyll maximum, weak spatial gradients, and irregular patterns. We highlight the temporal variability of these spatial patterns and the importance of anthropogenic and ~~climatic perturbations~~ environmental influences.

1 Introduction

As the most important energy source in aquatic systems, phytoplankton account for 1% of the global biomass but create around 50% of the global primary production (Boyce et al., 2010). Located at the land-ocean interface, estuarine-coastal systems, including estuaries, bays, lagoons, fjords, river deltas, and plumes, are relatively productive and abundant in phytoplankton (Carstensen et al., 2015). As the basis of the pelagic food web, phytoplankton have an immense impact on the biogeochemical cycles, water quality, and ecosystem services (Cloern et al., 2014). A sound understanding of the spatial

variability of phytoplankton is critical for effective assessment, exploitation, and protection of estuarine-coastal ecosystems but remains a challenge due to the complicated natural and anthropogenic controls (Grangeré et al., 2010; Srichandan et al., 2015).

The standing stock of phytoplankton is a function of sources and sinks that are subject to both biotic and abiotic influences (Lancelot and Muylaert, 2011; Jiang et al., 2015). Phytoplankton growth is regulated by bottom-up factors such as nutrients, light, and temperature (Underwood and Kromkamp, 1999; Cloern et al., 2014), while natural mortality and grazing pressure from zooplankton, suspension feeders, and other herbivores contribute to the loss of phytoplankton biomass (Kimmerer and Thompson, 2014). Physical transport can act as either a direct source or sink, driving algal cells into or out of a certain region (Martin et al., 2007; Qin and Shen, 2017). The hydrodynamic conditions also affect the phytoplankton biomass indirectly. For example, phytoplankton growth is dependent on transport of dissolved nutrients (Ahel et al., 1996). ~~concentrations of light-shading suspended particulate matter (SPM) are tightly associated with tide and wave motion~~ Tides and waves affect concentrations of light-shading suspended particulate matter (SPM) and thus photosynthesis (Soetaert et al., 1994). ~~stratification can considerably reduce the benthic filtration of the surface phytoplankton and change algal sedimentation~~ The efficiency of benthic filtration feeding on the surface phytoplankton is associated with stratification of the water column (Hily, 1991; Lucas et al., 2016).

For these reasons, the phytoplankton distribution in estuarine-coastal systems relies on the spatial patterns of physical, chemical, and biological environmental factors of each system (Grangeré et al., 2010). For example, phytoplankton variability in one semi-enclosed water body can be dominated by terrestrial input (river-dominated), oceanic input (tide-dominated), top-down effects (grazing-dominated), others, or a combination of the above factors. More often, it is the delicate balance of multiple factors that determine phytoplankton gradients. Under high river discharge, phytoplankton growth can be promoted by increasing nutrient input, whereas advective loss and high riverine SPM loading may inhibit algal enrichment (Lancelot and Muylaert, 2011; Shen et al., 2019). In tide-dominated systems, tides can resuspend SPM, negatively impacting phytoplankton, while at the same time bringing regenerated nutrients into the water column, or drive upwelling-induced algal blooms from the coastal ocean into estuaries (Sin et al., 1999; Roegner et al., 2002). Nitrate can support more phytoplankton biomass in microtidal estuaries than in macrotidal estuaries (Monbet, 1992). The relative importance of zooplankton and bivalve grazing on phytoplankton varies spatially (Kromkamp et al., 1995; Herman et al., 1999; Kimmerer and Thompson, 2014). These complexities make it challenging to discern the driving mechanisms of the spatial phytoplankton gradient, and comparative studies of different systems are lacking (Kromkamp and van Engeland, 2010; Cloern et al., 2017).

In situ observation, remote sensing, and numerical modeling are common techniques to reveal spatial patterns and detect their biophysical controls (Banas et al., 2007; Grangeré et al., 2010; Srichandan et al., 2015). Shipboard measurements of chlorophyll a (chl-a) provide a precise and dynamic assessment of the phytoplankton variability; however, the temporal (usually monthly) and spatial (usually tens of kilometers) resolutions are limited compared to satellite images and numerical models (Soetaert et al., 2006; Valdes-Weaver et al., 2006; van der Molen and Perissinotto, 2011; Cloern and Jassby, 2012;

2

Kaufman et al., 2017). Remote sensing of chl-a reveals the surface distribution with a sufficiently high spatial resolution and coverage, but only at favorable weather conditions (Srichandan et al., 2015). In comparison, ecological models are based on simplified assumptions and numerical formulations and cannot simulate every detail in natural process. However, a properly calibrated and validated model is capable of representing the interested system at a fine resolution (Friedrichs et al., 2018) and allows testing hypotheses of mechanisms driving the phytoplankton distribution (Jiang and Xia, 2017, 2018; Irby et al., 2018). As a reliable biophysical model must be based on observational and satellite data (Soetaert et al, 1994; Feng et al., 2015; Jiang et al., 2015), a combination of these approaches is optimal to improve our knowledge of the spatial heterogeneity in estuarine-coastal ecosystems.

In this study, we combined satellite, long-term monitoring, and numerical modeling to investigate the potential drivers of the spatial phytoplankton gradients in a well-mixed tidal bay, the Oosterschelde (SW Netherlands). In this case study, we identified the main environmental drivers of spatial phytoplankton distribution in the bay, and used some sensitivity model tests to quantify the impact of these drivers. Through such a mechanistic investigation into the spatial phytoplankton gradient, our case study was then used as a prototype in comparing spatial phytoplankton gradients among global estuaries and coastal bays. Based on a literature review, five main types of spatial heterogeneity in phytoplankton biomass are identified along with examples and dominant controls.

2 The study site

The Oosterschelde is located in the Southwest Delta of the Netherlands (Figure. 1). Due to the flood-protection constructions named Delta Works since the 1980s, the delta region has changed from an interconnected water network to individual water basins isolated by dams and sluices (Ysebaert et al., 2016). The confluence of the Rhine and Meuse Rivers flow into the North Sea through a narrow channel (Figure. 1) with a combined discharge of over 2000 m^3/s (Ysebaert et al., 2016). The Westerschelde (Figure. 1) is the only remaining estuary in the delta region covering fresh to saline waters (Ysebaert et al., 2016). With the freshwater input reduced to a negligible level compared to the tidal prism, the Oosterschelde has been filled with saline water (salinity 30–33), lost characteristics of an estuary, and developed into a tidal bay (Nienhuis and Smaal, 1994; Wetsteyn and Kromkamp, 1994). The northernmost end in the northern branch has salinities fluctuating between 28.5 and 30.5, caused by small freshwater inflow through the Krammer sluice. However, the occasional freshwater flux controlled by the sluice is mostly below 10 m^3/s (Ysebaert et al., 2016). This is negligible compared to the tidal exchange, which is ~2 × 10^4 m^3/s, estimated from a typical tidal prism of 9 × 10^8 m^3 in a 12-h tidal cycle. As part of the Delta Works, a partially-open storm surge barrier was implemented at the mouth of the Oosterschelde, which is occasionally closed during severe storms. Since then, the tidal basin still experiences a semi-diurnal tidal regime, but the average tidal range has been reduced by ~13% to 2.5–3.4 m from the west to east, the tidal flat area was reduced, and current velocity decreased (Nienhuis and Smaal, 1994; Vroon, 1994). In the post-barrier decades, the entire basin has been dominated by the

tidal exchange with the North Sea, causing net import of phytoplankton biomass and seston; the residence time of the bay ranges 0–150 days from the western to eastern ends (Jiang et al., 2019a).

The phytoplankton composition in the Oosterschelde has also changed since the Delta Works: the previously dominating diatoms have decreased, while the small flagellates and weakly silicified diatoms became more abundant, especially in summer (Bakker et al., 1994). The annual cycle of phytoplankton biomass is characterized by a spring bloom and a much weaker late summer peak (Wetsteyn and Kromkamp, 1994). The Oosterschelde is extensively used for aquaculture of Pacific oysters (*Crassostrea gigas*) and blue mussels (*Mytilus edulis*) in the past decades, and their annual productions are approximately 3 and 20–40 kt fresh weight, respectively (Smaal et al., 2009; Wijsman et al., 2019). Oysters, mussels, and wild cockles (*Cerastoderma edule*) are the main benthic suspension feeders in the basin (Figure. 1). Strong pelagic-benthic coupling has been reported for the Oosterschelde ecosystem: benthic filtration very likely accounts for the declining annual primary production, while phytoplankton growth is stimulated by bivalve regenerated nutrients (Smaal et al., 2013). In addition, abundant benthic suspension feeders make the Oosterschelde an important feeding ground and international conservation zone for wading birds (Tangelder et al., 2012).

3 Methods

3.1 Field observations

From 1995 to 2013, the Royal Netherlands Institute for Sea Research (NIOZ) conducted shipboard monitoring of the Oosterschelde on a biweekly to monthly basis. The monitoring campaign routinely collected water samples at eight stations in the basin (OS1–OS8, Figure. 2) for nutrient measurements and filtered them for measurements of chl-a and SPM. The Dutch government agency Rijkswaterstaat (RWS) has monitored nutrients and chl-a in the Oosterschelde at different locations (e.g., RWS1–RWS4, Figure. 2), and these monthly data are freely accessible on the RWS data portal (https://waterinfo.rws.nl). Compared with the NIOZ data, the RWS data include two offshore stations RWS1 and RWS2 (Figure. 2). Since the study region is mostly well-mixed (Wetsteyn and Kromkamp, 1994), both datasets used surface samples to represent the water column at each station.

Primary production was estimated by $^{14}CO_2$ uptake (mg-C h^{-1}) during two-hour incubation experiments for all 16 NIOZ sampling dates in 2010 at stations OS2 and OS8 (Fig. 2), by the C14 method. A *PI*-curve linking irradiance (I, μmol-photons m^{-2} s^{-1}) to the chl-a normalized C-fixation rate (P, mg-C mg-chl-a^{-1} h^{-1}) was mathematically represented by a maximum C-fixation rate (P_m, mg-C mg-chl-a^{-1} h^{-1}), an initial slope of the curve (α, mg-C mg-chl-a^{-1} h^{-1}/μmol-photons m^{-2} s^{-1}) and the irradiance at which P_m was optimal occurred (I_{opt}, μmol-photons m^{-2} s^{-1}) according to the model of Eilers and Peeters (1988). Light intensity at multiple water depths was measured in the field with Licor LI-192SB cosine-corrected light sensors connected to a Licor LI-185B quantum meter Light attenuation was measured to estimate the light extinction coefficient K_d (m^{-1}) and generate the light attenuation curve $I_z = I_0 \exp(-zK_d)$, where I_0 and z are surface light intensity and water depth, respectively. With the hourly photosynthetically active radiation (PAR) measured at the NIOZ as I_0, the hourly

PAR (I_z) throughout the water column was computed. For a full description, see Kromkamp and Peene (1995). Then, with P_m, α, I_{opt}, and I available, the hourly photosynthetic rate at each water depth (P_z) was calculated and integrated over depth to obtain the primary production of the entire water column and during the whole day. We used the measured ~~values~~ primary production data without estimating the respiratory losses as respiration will not affect the N-content of the algae. In a short

5   incubation time, the C14 method is often thought to reflect gross primary productivity (*GPP*). However, results by Halsey et al. (2010, 2013) showed that even a 30 min C14 incubation experiment can reflect *GPP* at low growth rates and net primary productivity (*NPP*) at high growth rates. Hence, as during the main growing seasons growth rates are generally high (Underwood and Kromkamp, 1999), we assume that our C14-method reflects *NPP* measurements.

3.2 Numerical modeling

10   A three-dimensional hydrodynamic-biogeochemical model GETM-FABM (General Estuarine Transport Model coupled with the Framework for Aquatic Biogeochemical Models) was applied in a two-year (2009–2010) simulation to identify drivers of spatial phytoplankton dynamics in the Oosterschelde. GETM and FABM are open-source models, available from websites https://getm.eu/ and https://github.com/fabm-model/fabm. The model was implemented on a 300 m × 300 m rectangular grid with 10 equally-divided vertical layers, covering the Oosterschelde and part of the North Sea

15   (Fig~~ure~~. 1). The hydrodynamic model using GETM version 2.5.0 is driven by realistic meteorological forcing (winds, irradiance, air pressure, etc.) and tides and the output water level, temperature, salinity, and current velocity are calibrated and validated with observational data (Jiang et al., 2019a). Jiang et al. (2019a) provide a detailed description of the GETM setup and model ~~verification~~ validation. The validation of FABM is presented in Section 4.2.

      The biogeochemical model is coupled online with GETM on the FABM platform (Bruggeman and Bolding, 2014).
20   The physical and biogeochemical simulations were conducted simultaneously with a time step of 8 s. In each time step, GETM provides FABM with the environmental variables, such as temperature, water elevation, and irradiance. The transport and mixing of nutrients, detritus, and plankton biomass is represented by the same equation as that of salinity except that phytoplankton and detritus sink at a speed of 0.2 m ~~per day~~ d^{-1} and 1.0 m d^{-1}, respectively (Eppley et al., 1967; Soetaert et al., 2001).

25   Our biogeochemical model is nitrogen-based and consists of a pelagic and benthic module (Fig~~ure~~. 3). The pelagic module is a typical NPZD framework comprising the state variables Nutrient (DIN, dissolved inorganic nitrogen), Phytoplankton, Zooplankton, and Detritus (unit: mmol nitrogen m^{-3}), while the benthic variables in mmol nitrogen m^{-2} include benthic detritus, microphytobenthos, and the three dominant bivalve species in the Oosterschelde: mussels, oysters and cockles. The main formulations, variables, and parameters are summarized in Tables 1 and 2. The climatological data in

30   December and January averaged using the 19-year observations is used as the initial model condition. The shellfish distribution (see Fig~~ure~~. 1) and annual biomass in 2009 and 2010 are estimated by Wageningen Marine Research (Smaal et al., 2013; Jiang et al., 2019a). The model output is compared with available observational DIN, chl-a, and *NPP* described in Section 3.1. Given that *NPP* was measured by carbon-based methods, the nitrogen-based simulation results were converted

to carbon using the Redfield ratio (C:N = 6.625 mol C mol N^{-1}). Phytoplankton biomass was measured in Chlorophyll units. We have prescribed a Chl:N ratio (Chl:N = 2 mg Chl mmol N^{-1}, Soetaert et al., 2001) to compare our model output to the chlorophyll data.

In order to investigate the roles of coastal influx and benthic grazing in shaping the spatial phytoplankton patterns in the basin, we conducted two idealized numerical scenarios in addition to the realistic (baseline) run. One scenario is halving the DIN concentration and phytoplankton biomass at the open boundary (i.e., the North Sea including the Westerschelde and Rhine river plumes, see Figure. 1). The other scenario switched off the bivalve state variables. Based on our assessment, the effects of freshwater input on DIN and chl-a are minimal, local, and far less significant than the above two factors. Thus, the sensitivity runs of the freshwater input will not be elaborated hereafter.

3.3. Satellite remote sensing

A clear sky Sentinel-2 MSI (10 m spatial resolution) satellite image of 11 May 2018 (10:55 UTC) for tile 31UET was downloaded as level 1C data from the Copernicus Sentinel hub (https://scihub.copernicus.eu). The Acolite processor (version Python 20190326.0) developed by RBINS (Vanhellemont and Ruddick, 2016) was applied using default settings to correct for atmospheric (aerosol) effects based on a dark spectrum fitting (Vanhellemont and Ruddick, 2018; Vanhellemont, 2019), to flag clouds and land, and to retrieve L2W water quality parameters from water reflectance, i.e., concentrations of chl-a and SPM. Chl-a was retrieved using the red edge algorithm defined by Gons et al. (2002) with a mass specific chl-a absorption set to 0.015. SPM was retrieved using the (red band) algorithm defined by Nechad et al. (2010) and recalibrated in 2016 for Sentinel-2 MSI. Data were extracted in the Sentinel Application Platform (SNAP version 7.0.0) and converted to GeoTIFF for further processing in ArcGIS. The satellite image was acquired during high water: water level at Rijkswaterstaat tide gauge station Stavenisse (https://waterinfo.rws.nl/%20/nav/index) was +1.12 m NAP incoming tide during overpass. A Sentinel-2 MSI image of 21 April 2019 (10:56 UTC) was acquired during low water conditions (i.e., such as -1.58m NAP incoming tide), and processed in the same way. "Land" flags obtained from this low water image were used to further flag shallow waters (i.e., the inundated tidal flats) in the highwater image, to avoid potential bottom reflectance.

4 Results

4.1 Field observations

The 19-year chl-a time series illustrates the seasonal pattern of phytoplankton biomass in the Oosterschelde (Figure. 4). The spring bloom takes place in March or April during conditions of increasingly favorable temperature, light, and nutrients and lasts less than a month. The peak biomass varies dramatically interannually (Fig. 5), with smaller peaks during different months, especially in 2010 (Fig. 4). Likely due to nutrient limitation and grazing pressure, the summer biomass stays mostly below 10 mg m^{-3} (Figs. 4 and 5). In the well-mixed Oosterschelde with limited freshwater input, temperature

and light constrain algal growth in winter, when nutrients accumulate and phytoplankton biomass falls below 3 mg m^{-3} (Figs. 4 and 5). These seasonal controls of phytoplankton variability are substantiated with the numerical model in Section 4.2.

To better display the spatial chl-a gradients, ~~the time series is zoomed in to four years 2007–2010~~ monthly averages and standard deviations of the 19-year observations are displayed (Figure. 5). A decreasing chl-a gradient from the mouth (OS1) to head (OS8) of the basin is observed mainly during the spring bloom, whereas the spatial phytoplankton gradient is not as pronounced in summer and winter (Figure. 5a). The station RWS1 that is close to the mouth of the Westerschelde estuary usually has a higher chl-a concentration than further offshore (RWS2) and in the Oosterschelde (RWS3 and RWS4) (Figure. 5b). Despite interannual variability in the timing of the bloom and different sampling time every year, the period March to May mostly covers the initiation, development, and wane of the spring bloom. The 19-year average phytoplankton biomass during this season demonstrates a clear gradient in the bay and adjacent coastal sea (Figure. 2). The chl-a decreases from the Westerschelde plume region (RWS1) offshore (RWS2) and further into the eastern and northern ends of the Oosterschelde (Figure. 2).

4.2 Numerical modelling

The model results compared to observed concentrations of DIN and chl-a in a two-year simulation are shown in Figure. 6. Most DIN consumption happens during the spring bloom, and the regenerated DIN accumulates over winter until the next bloom sets off. The simulated chl-a during the bloom demonstrates the same gradient between the western and eastern bay as observed (OS1 > OS3 > OS8, Figures. 6d–6f). The model skill is quantified by correlation coefficients (CC = 0.94 for DIN and 0.81 for chl-a) and root mean square errors ($RMSE$ = 6.0 mmol m^{-3} for DIN and 3.9 mg m^{-3} for chl-a) between simulation and observation. Despite capturing the major seasonal and spatial patterns, the model seems to miss some details such as overestimating the recycled DIN at OS8 and showing a slower collapse of spring blooms than observed. Meanwhile, the daily time series of the model output exhibits spring-neap biweekly fluctuations (Figure. 6) that cannot be substantiated by the observations owing to a low sampling frequency.

The modeled NPP, the product of phytoplankton biomass and growth rate, is in general agreement with the measurements (Figure. 7, black line). According to Equation (2) in Table 1, the growth rate is a function of temperature, nutrient, and light factors in the model. Here we decompose the seasonal cycle of these three factors and use their product to assess the growth rate (Fig. 8). Before the bloom, both phytoplankton biomass and growth rate are low, resulting in a low NPP (Figs. 7 and 8). The fast-growing period, around Day 100 as a consequence of increased temperature and light (Figs. 7 and 8), triggers the increase in biomass that leads to the bloom. The spring bloom is terminated due to enhanced nutrient limitation around Day 125 (Figs. 7 and 8). In the low-biomass post-bloom summer (Figure. 6), both modeled and measured NPP is only slightly lower than that in the bloom (Figure. 7) and the environmental conditions are still favorable for growing (Fig. 8)~~, indicating that the growth rate is still high~~. ~~This~~ The summer growth rate is mainly fueled by regenerated nutrients, while the low biomass results substantially from grazing. The model underestimated DIN and thus NPP after the spring bloom (Days 490–540 in Fig. 6 and 125–175 in Fig. 7) and overestimated the recycled DIN at OS8 in fall 2010 (Days 600–

7

650 in Figure. 6a), which explains the overestimation of *NPP* in this period (Days 235–285 in Figure. 7a). The observed and simulated *NPP* at OS8 (902.6 ± 928.4 mmol C m^{-2} d^{-1} and 1033.9 ± 1084.3 mmol C m^{-2} d^{-1}, respectively) is generally higher than that at OS2 (Figure 7 722.5 ± 794.6 mmol C m^{-2} d^{-1} and 606.0 ± 499.5 mmol C m^{-2} d^{-1}, respectively). According to the one-tail t-test, the difference between observed *NPP* at these two stations is not significant ($t = 0.59$, $p > 0.05$, $n = 16$), whereas due to the overestimation the simulated *NPP* at OS 8 is significantly higher than that at OS2 ($t = 6.85$, $p < 0.05$, $n = 365$). This is in contrast to the chl-a, which is higher at OS2 (Figure. 2).

The calibrated and validated model was used to map the 15-day average chl-a during the peak bloom in 2009 (Figure. 89). The North Sea exhibits significantly higher algal biomass than the Oosterschelde (Figure. 89). Inside the bay, phytoplankton biomass is clearly low over the shellfish-colonized area (compare Figures. 1 and 8). The north-south and east-west chl-a gradients observed in field monitoring data are reproduced in the model results (Figures. 2 and 89).

When switching off bivalve activities, the modeled phytoplankton biomass significantly increases, especially at the eastern station OS8 (Figure. 910). At this station, the chl-a during the bloom is nearly tripled, it doubled at OS3 and increased by 20% at OS1, respectively (Figure. 910). The west to east spatial chl-a gradient is weakened in spring and even reversed in summer, i.e., concentrations decrease seawards (Figure. 910). Remarkably, without bivalves, the summer *NPP* at OS8 is not greatly affected (Figure. 7a) despite increased algal biomass, which implies a reduction in the growth rate (*DinUpt* in Equation (2), Table 1). Given the unchanged light and temperature in the no-bivalve scenario, the reduced growth rate results from diminished nutrient regeneration. The summer *NPP* at OS2 is increased when bivalves are turned off (Figure. 7b), which is a consequence of increased phytoplankton biomass.

Halving the DIN and phytoplankton loading from the North Sea hardly has an influence on the *NPP* in the Oosterschelde (Figure. 7). This indicates that allochthonous coastal nutrients are not a major source of inner-bay primary production, which relies mainly on recycling. With halved coastal import, the modeled peak phytoplankton biomass is nearly halved at OS1, but the reduction is lower at OS3 (~35%) and OS8 (~20%) (Figure. 910). Therefore, tidal import has its impact mainly exclusively near the bay mouth during the bloom. This contrasts to the benthic bivalves that exert grazing pressure all over the bay and stimulates primary production by replenishing inorganic nutrients into the water column, the latter process being crucial in nutrient-depleted seasons.

4.3 Satellite remote sensing

Remote sensing images with sufficient spatial resolution, in this case the Sentinel-2 MSI data, are utilized to complement the spatial patterns shown in observational and modeling data. In an attempt to find images during the spring bloom and high tide (to avoid interference from bottom reflectance), we only found one post-bloom snapshot under clear sky (Figure. 101a). This provides additional insight into the observed and modeled spatial chl-a pattern. On 11 May 2018, the chl-a concentration was highest in the central basin and reduced eastwards and northwards into the highly bivalve-populated areas (Figures. 1 and 101a), consistent with the chl-a gradient described in Sections 4.1 and 4.2. However, the post-bloom chl-a concentration was low in the North Sea so that low import was shown in the southwestern bay near the mouth (Figures.

10̶1a). Such a spatial chl-a pattern with higher concentrations in the central basin (Fig̶u̶r̶e̶. 10̶1a) is often present in the model results. For example, in the post-bloom period in 2008 and 2009, the chl-a concentration at OS3 is higher than OS1 and OS8 at times (Fig̶u̶r̶e̶. 5a). Likewise, in a post-bloom model snapshot during high tide on 1 May 2010 (Fig̶u̶r̶e̶. 10̶1b), the phytoplankton distribution exhibits a similar spatial gradient as in Fig̶u̶r̶e̶. 10̶1a.

5 Discussion

The approaches applied in this case study including field observation, numerical modeling, and satellite remote sensing each have their drawbacks. The monitoring data is not frequent enough to capture the peak bloom that lasts only a couple of weeks and misses details in spatial distribution between stations. The temporal resolution of the satellite data is even lower, but the spatial detail is very high. The model, while resolving spatial and temporal scales at a high resolution, is based on simplified assumptions. The NPZD model considers nitrogen only and assumes no phosphorus or silicon limitation in phytoplankton growth. In late spring, phosphorus or silicon may become limited in the Oosterschelde (Smaal et al., 2013; Wetsteyn and Kromkamp, 1994). This likely explains the faster DIN consumption in the simulated data compared to the observation (Fig̶u̶r̶e̶. 6a–6c), resulting in the accelerated nitrogen limitation and underestimation of the post-bloom *NPP* (Figs. 7 and 8). Additionally, our model does not account for the shellfish harvest, mostly in late summer, which can contribute to the overestimation of the regenerated DIN and hence NPP, especially in the eastern part (e.g., Fig̶u̶r̶e̶s. 6a and 7a). When converting the nitrogen-based model results to compare with chl-a and the carbon-based *NPP*, the Chl:N and Redfield ratios were applied, without considering the variable stoichiometry in natural phytoplankton groups. Despite these simplifications and limitations, the approaches complement each other in the spatiotemporal resolution and coverage and offer insight into the phytoplankton distribution in the Oosterschelde, as well as the underlying mechanisms.

Grazing by filtration feeders is found to be the dominant factor shaping the spatial and seasonal phytoplankton patterns in the Oosterschelde. In the eastern and northern bay, the residence time is relatively long (>100 days, estimated by the e-folding method and the remnant function by Jiang et al., 2019b), a̶n̶d̶ ̶t̶h̶e̶ ̶w̶a̶t̶e̶r̶ ̶c̶o̶l̶u̶m̶n̶ ̶i̶s̶ ̶w̶e̶l̶l̶ ̶m̶i̶x̶e̶d̶, water depth and cross-bay area are much smaller, and the tidal amplitude and mixing are stronger due to geometric convergence (Jiang et al., 2020), which contributes to stronger pelagic-benthic coupling and creates favorable feeding conditions for suspension feeders (Hilly, 1991). Thus, over and near the shellfish habitat, the phytoplankton biomass is usually low, even during the bloom (Fig̶u̶r̶e̶s. 1 and 8̶9). Smaal et al. (2013) attributed the decline of the annual primary production and chl-a concentration in the Oosterschelde to overgrazing, as found in the Bay of Brest (Hilly, 1991) and many Danish estuaries (Conley et al., 2000). Our findings support the predominant top-down control on phytoplankton distribution and standing stocks (Fig̶u̶r̶e̶. 9̶10), as well as on primary production, particularly in the post-bloom seasons (Fig̶u̶r̶e̶. 7b). It has been shown that a recruitment failure of mussels and cockles promotes primary production and algal accumulation in the Dutch Wadden Sea (Beukema and Cadée, 1996), consistent with our numerical experiment removing bivalves. Although bivalves accelerate nutrient remineralization, this positive feedback on phytoplankton growth does not compensate for the grazing loss.

Optimization of the bivalve stock size and culture locations based on these scientific insights could enhance phytoplankton proliferation and increase the shellfish carrying capacity.

Compared to benthic feeding, tidal import mainly influences the phytoplankton biomass in the southern channel near the mouth. The Southern Bight of the North Sea, and more particular the water in river plumes (e.g., Westerschelde and Rhine plumes), is relatively productive, compared to other shelf seas (van der Woerd et al., 2011). The spring bloom in the Oosterschelde is usually not as strong as in the adjacent North Sea (Figures. 2, 5, and 89), so that tidal import of phytoplankton from the North Sea sets the upper limit of the phytoplankton in the Oosterschelde (Figure. 910).

Note that the observed seaward increasing phytoplankton biomass is not so pronounced in each of the 19 years, such as in 1997 and 2012 in Fig. 4a. The interannual variability of the spring bloom timing and magnitude is among the potential causes. In winter and early spring, the shallower and landlocked Oosterschelde may be warmed up a few days faster than the adjacent North Sea, which may result in earlier spring bloom at the landward end in some years, such as 1996, 1997, and 2005 shown in Fig. 4b. Thus, the resultant spatial chl-a distribution may differ if the sampling activity is conducted during or between these two bloom windows. Given the relative low sampling frequency (every month or two weeks), different observational activities may change the spatial chl-a distribution (e.g., Year 2010 in Figs. 5a and 5b). Additionally, if the bloom is of similar magnitude in and out of the bay, the spatial gradient may not be as strong, such as in 2012 in Fig. 4a. Therefore, in consideration of the interannual variability of the spring blooms and the possible mismatch with sampling campaigns, the observational spatial phytoplankton gradient may be inconspicuous in certain years but evident over the long term (Figs. 2 and 5).

6 Synthesis

The Oosterschelde represents a land-ocean transitional system that is shallow, dynamic, and driven by pelagic-benthic coupling and exchange with the sea. The grazing pressure increases into the bay because of reduced water depth and increasing bivalve biomass, and residence time, tidal mixing, and thus pelagic-benthic coupling, while the North Sea, having with higher phytoplankton biomass is a phytoplankton source. As a result, the phytoplankton concentration during the spring bloom consistently declines from the seaward to the landward end. When halving the nutrient and algal loading from the North Sea, the phytoplankton gradient in spring is not as pronounced, although still decreasing toward the landward end (Figure. 112). Without the grazing sink however, the phytoplankton distribution tends to be spatially uniform (Figure. 112). Given the temporal variability of dominant environmental factors, the phytoplankton gradient also changes over time. In the post-bloom period for instance, chl-a may exhibit a central maximum, or it may exhibit a constant concentration in winter. This shows that the spatial gradient of phytoplankton biomass in estuarine-coastal systems depends on the relative importance of the main drivers of phytoplankton accumulation. Based on a literature review, we can roughly divide estuarine coastal systems into five major types Associated with the respective dominant environmental drivers, we compare

the Oosterschelde case with other estuarine-coastal systems and summarize five common spatial phytoplankton patterns (Fig~~ure~~. 1~~2~~3).

~~Type I systems exhibit~~ Increasing phytoplankton biomass from the landward to seaward ends (Type I, Fig~~ure~~. 1~~2~~3). ~~Such a simple gradient~~ can often be ascribed to an increasing source from the seaside, an increasing sink landwards, or more favorable growth conditions towards the sea. The Oosterschelde is a typical example ~~with Type I phytoplankton distribution~~ during the spring bloom (Fig~~ure~~. 8), shaped by both marine input and increasing benthic filtration landward. The seawards increasing gradient is also common in estuaries and bays open to coastal upwelling zones (e.g., the Rías Baixas of Galicia and Tomales Bay), where algal blooms generated during upwelling events are transported into bays via multiple physical mechanisms including tidal stirring and gravitational and wind-driven circulation (Figueiras, et al., 2002; Hickey and Banas, 2003; Martin et al., 2007). In contrast, phytoplankton in the Chilika Lagoon is mostly light-limited due to the massive riverine sediment loading. Here it is a seaward increase in water transparency that leads to increasing chl-a concentrations (Srichandan et al., 2015). Hence, ~~the same type of~~ similar phytoplankton gradients may be driven by distinct mechanisms in various systems.

Contrary to the Oosterschelde case, phytoplankton biomass ~~decreasing~~ decreases in the seaward direction in some systems ~~is named~~ (Type II, ~~(~~Fig~~ure~~. 1~~2~~3). A typical example is the Scheldt River and Westerschelde Estuary, a eutrophic and turbid estuary with salinity ranging 0–30 (Soetaert et al., 2006). Numerical models and field observation reveal that the chl-a concentration is highest in the tidal fresh portion, reduces sharply between salinity 5–10, and ~~maintains~~ is maintained at a lower level towards the polyhaline region (Soetaert et al., 1994; Kromkamp et al., 1995). The high phytoplankton biomass in the upper reach is a result of tributary import, high nutrient levels, and lack of zooplankton grazers, whereas the increasing salinity stress on the freshwater species and grazing pressure in the mesohaline zone suppress the phytoplankton proliferation (Soetaert et al., 1994; Kromkamp and Peene, 1995; Muylaert et al., 2005). Similar seawards decreasing phytoplankton gradient is also found in many river and estuarine plumes (Fig~~ure~~. 1~~2~~3), where the nutrient gradient controls the phytoplankton distribution (Gomez et al., 2018; Jiang and Xia, 2018).

A chl-a maximum zone (CMZ) occurs in many estuaries with substantial freshwater input ~~and we classify it as~~ (Type III in ~~(~~Fig~~ure~~. 1~~2~~3). Taking the Chesapeake Bay as an example, the upper bay is characterized by high terrestrial sediment concentrations and strong light limitation for phytoplankton growth (Son et al., 2014). A turbidity maximum zone is located near the front of salt intrusion (North et al., 2004). Beyond this location, the CMZ appears in the middle reach (Jiang and Xia, 2017), while nitrogen limitation is constantly detected in the lower bay (Miller and Harding, 2007). The CMZ is a combined consequence of the optimal light conditions and abundant terrestrial nutrients, and the CMZ location and coverage shift with river discharge and weather (Fisher et al., 1988; Miller and Harding, 2007). In some other estuaries with a CMZ (e.g., the Neuse-Pamlico estuary and York River), owing to a narrow river channel and high discharge, the flushing rate in the upper estuary can be faster than the phytoplankton turnover rate, which, rather than light, limits phytoplankton accumulation (Sin et al., 1999; Valdes-Weaver et al., 2006). In these systems, the CMZ is always in wider reaches with sufficiently long residence time (Valdes-Weaver et al., 2006).

If the transport loss is higher than the growth rate in the entire basin, the phytoplankton biomass is low everywhere and negatively correlated with the flow velocity (Type IV, Fig~~ure~~. 1~~2~~3). The Hudson River estuary is one of such estuaries with high nutrient loading but low and hardly spatially variable chl-a (Howarth et al., 2000). After the colonization of the invasive zebra mussel (*Dreissena polymorpha*) in the 1990s, grazing and transport losses are two dominant sink terms maintaining a low basin-wide phytoplankton standing stock in the estuary (Strayer et al., 2008). Similarly, due to the invasive clam *Potamocorbula amurensis*, the San Francisco Bay witnessed a five-fold drop in chl-a and the suppression of zooplankton, and higher trophic levels (Cloern and Jassby, 2012; Lucas et al., 2016). The phytoplankton gradient has changed from Types III to IV (Cloern et al., 2017)~~. Hence, the Type IV phytoplankton gradient~~, which is generally associated with strong sink factor(s) distributed all over the system.

The dominant sink (or source) factor is not always distributed uniformly nor does it follow consistent gradients in estuarine-coastal systems, generating irregular phytoplankton distribution (Type V, Fig. 13). For instance, in the Baie des Veys estuary, benthic grazing by cultivated oysters results in an area of low chl-a concentrations over the oyster bed, and this patch of low chl-a is imposed onto a seawards decreasing chl-a gradient, forming an irregular spatial pattern (Grangeré et al., 2010). In the Krka estuary, an untreated sewage discharge acts as a DIN point source, increasing the phytoplankton production downstream. Without the point source, phytoplankton seem to follow a Type II gradient (Ahel et al., 1996). In the St. Lucia estuary, controls of primary production include nutrient stoichiometry, temperature, irradiance, and hydrological changes which all vary in different sub-regions and render complex spatial heterogeneity in phytoplankton distribution (van der Molen and Perissinotto, 2011). ~~Herein, we summarize all irregular phytoplankton patterns into Type V (Figure 12).~~

7 Summary

In the Oosterschelde, a tidal bay along the North Sea, we detect a seaward increasing phytoplankton gradient in the two-decade monitoring data. This spatial chl-a pattern was also reproduced with a nitrogen-based NPZD model calibrated and verified with observational data. In an effort to understand the main drivers of such a phytoplankton gradient, two experimental model runs were performed: switching off bivalve filtration and halving the nutrient and phytoplankton concentrations in the North Sea boundary, respectively. Results indicate that the landward increasing benthic grazing pressure is the primary cause of the spatial phytoplankton gradient, while import from the North Sea tends to strengthen the gradient. The satellite image implies that tidal import is mainly influential in the southwestern bay. With the variation of these two drivers, the spatial phytoplankton distribution varies seasonally.

In a synthesis of the literature, we made an inventory of how the spatial phytoplankton gradient in estuarine-coastal systems is shaped by the distribution of the main environmental drivers. Five common types of spatial phytoplankton patterns ~~are identified:~~ include seawards increasing, seawards decreasing, concave with a chlorophyll maximum, weak spatial gradients, and irregular patterns. ~~It can be inferred from the temporal variation of spatial phytoplankton heterogeneity in the Oosterschelde that processes over event (e.g., tropical cyclones), seasonal (e,g., monsoon), interannual (e.g., wet vs.~~

dry years), and decadal (e.g, climate change) scales can extensively change the structure of the lower food. Through this study and the review of other systems, we also underline the role of phytoplankton as an ecosystem indicator of anthropogenic (e.g., aquaculture, invasive species) and climatic (e.g., global warming) disturbance. It should be noted the spatial phytoplankton pattern is subject to temporal changes and cannot be discussed without specifying the temporal window. For example, the spatial chl-a gradient in this study is different before, during, and after the spring bloom and subject to substantial interannual variability; in river-dominated systems (Fig. 13), phytoplankton distribution is usually regulated by the episodic, seasonal, and interannual variations of river discharge (Kromkamp and van Engeland, 2010). In addition to natural changes, phytoplankton abundance and spatial heterogeneity can reflect how the lower trophic levels are affected by anthropogenic influences and stressors, such as aquaculture (this study), invasive species (Cloern et al., 2017), and coastal engineering works (Wetsteyn and Kromkamp, 1994).

Code and data availability

The codes for GETM and FABM models are open-access on https://getm.eu/ and https://sourceforge.net/projects/fabm/, respectively. The RWS observational data is accessible on https://www.rijkswaterstaat.nl/water. The NIOZ monitoring data is archived on the NIOZ data repository and available upon request. The satellite data can be downloaded from the Copernicus Sentinel hub (https://scihub.copernicus.eu).

Author contributions

LJ ran the simulations, analyzed the results, and initiated the writing of the manuscript. TG and KS provided guidance and important insights into data interpretation. JCK measured the primary production using the $^{14}CO2$ uptake experiment. DvdW analyzed the satellite data. JCK and DvdW offered important insight into the phytoplankton dynamics. PMCDLC and KS built a 1D NPZD model as a basis of the 3D setup. All authors participated in the writing and editing of the manuscript.

Competing interests.

No competing interests are present.

Acknowledgments

References

Ahel, M., Barlow, R. G., and Mantoura, R. F. C.: Effect of salinity gradients on the distribution of phytoplankton pigments in a stratified estuary, Mar. Ecol. Prog. Ser., 143, 289–295, http://doi.org/10.3354/meps143289, 1996.

Bakker, C., Herman, P. M. J., and Vink, M.: A new trend in the development of the phytoplankton in the Oosterschelde (SW Netherlands) during and after the construction of a storm-surge barrier, Hydrobiologia, 282/283, 79–100., http://doi.org/10.1007/BF00024623, 1994.

Banas, N. S., Hickey, B. M., Newton, J. A., and Ruesink, J. L.: Tidal exchange, bivalve grazing, and patterns of primary production in Willapa Bay, Washington, USA, Mar. Ecol. Prog. Ser., 341, 123–139, http://doi.org/10.3354/meps341123, 2007.

Beukema, J. J., and Cadée, G. C.: Consequences of the sudden removal of nearly all mussels and cockles from the Dutch Wadden Sea, Mar. Ecol., 17, 279–289, http://doi.org/10.1111/j.1439-0485.1996.tb00508.x, 1996.

Boyce, D. G., Lewis, M. R., and Worm, B.: Global phytoplankton decline over the past century, Nature, 466, 591–596, http://doi.org/10.1038/nature09268, 2010.

Bruggeman, J., and Bolding, K.: A general framework for aquatic biogeochemical models. Environ, Modell. Softw., 61, 249–265, http://doi.org/10.1016/j.envsoft.2014.04.002, 2014.

Carstensen, J., Klais, R., and Cloern, J. E.: Phytoplankton blooms in estuarine and coastal waters: Seasonal patterns and key species, Estuar. Coast. Shelf Sci., 162, 98–109, http://doi.org/10.1016/j.ecss.2015.05.005, 2015.

Cloern, J. E., Foster, S. Q., and Kleckner, A. E.: Phytoplankton primary production in the world's estuarine-coastal ecosystems, Biogeosciences, 11, 2477–2501, http://doi.org/10.5194/bg-11-2477-2014, 2014.

Cloern, J. E., and Jassby, A. D.: Drivers of change in estuarine-coastal ecosystems: Discoveries from four decades of study in San Francisco Bay, Rev. Geophys., 50, http://doi.org/10.1029/2012RG000397, 2012.

Cloern, J. E., Jassby, A. D., Schraga, T. S., Nejad, E., and Martin, C.: Ecosystem variability along the estuarine salinity gradient: Examples from long-term study of San Francisco Bay, Limnol. Oceanogr., 62, S272–S291, http://doi.org/10.1002/lno.10537, 2017.

Conley, D. J., Kaas, H., Møhlenberg, F., Rasmussen, B., and Windolf, J.: Characteristics of Danish estuaries, Estuaries, 23, 820–837, http://doi.org/10.2307/1353000, 2000.

Eilers, P. H. C., and Peeters, J. C. H.: A model for the relationship between light intensity and the rate of photosynthesis in phytoplankton, Ecol. Model., 42, 199–215, http://doi.org/10.1016/0304-3800(88)90057-9, 1999.

Eppley, R. W., Holmes, R. W., and Strickland, J. D. H.: Sinking rates of marine phytoplankton measured with a fluorometer, J. Exp. Mar. Biol. Ecol., 1, 191–208, https://doi.org/10.1016/0022-0981(67)90014-7, 1967.

Feng, Y., Friedrichs, M. A. M., Wilkin, J., Tian, H., Yang, Q., Hofmann, E. E., Wiggert, J. D., and Hood R. R.: Chesapeake Bay nitrogen fluxes derived from a land-estuarine ocean biogeochemical modeling system: Model description, evaluation, and nitrogen budgets, J. Geophys. Res. Biogeosci., 120, 1666–1695, http://doi.org/10.1002/2015JG002931, 2015.

Figueiras, F. G., Labarta, U., and Reiriz, M. F.: Coastal upwelling, primary production and mussel growth in the Rías Baixas of Galicia, Hydrobiologia, 484, 121–131, http://doi.org/10.1007/978-94-017-3190-4_11, 2002.

Fisher, T. R., Harding Jr, L. W., Stanley, D. W., and Ward, L. G.: Phytoplankton, nutrients, and turbidity in the Chesapeake, Delaware, and Hudson estuaries, Estuar. Coast. Shelf Sci., 27, 61–93, http://doi.org/10.1016/0272-7714(88)90032-7, 1988.

5 Friedrichs, M. A., St-Laurent, P., Xiao, Y., Hofmann, E., Hyde, K., Mannino, A, Najjar, R. G., Narváez, D. A., Signorini, S. R., Tian H., Wilkin, J., Yao, Y., Xue, J.: Ocean circulation causes strong variability in the Mid-Atlantic Bight nitrogen budget, J. Geophys. Res. Oceans, 124, 113–134, https://doi.org/10.1029/2018JC014424, 2018.

Gomez, F. A., Lee, S. K., Liu, Y., Hernandez Jr, F. J., Muller-Karger, F. E., and Lamkin, J. T.: Seasonal patterns in phytoplankton biomass across the northern and deep Gulf of Mexico: a numerical model study, Biogeosciences, 15, 3561–
10 3576, http://doi.org/10.5194/bg-15-3561-2018, 2018.

Gons, H. J., Rijkeboer, M., and Ruddick, K. G.: A chlorophyll-retrieval algorithm for satellite imagery (medium resolution imaging spectrometer) of inland and coastal waters, J. Plankton Res., 24, 947–951, http://doi.org/10.1093/plankt/24.9.947, 2002.

Grangeré, K., Lefebvre, S., Bacher, C., Cugier, P., and Ménesguen, A.: Modelling the spatial heterogeneity of ecological
15 processes in an intertidal estuarine bay: dynamic interactions between bivalves and phytoplankton, Mar. Ecol. Prog. Ser., 415, 141–158, http://doi.org/10.3354/meps08659, 2010.

Halsey, K. H., Milligan, A. J., and Behrenfeld, M. J.: Physiological optimization underlies growth rate-independent chlorophyll-specific gross and net primary production. Photosynth, Res., 103, 125–137, http://doi.org/10.1007/s11120-009-9526-z, 2010.

20 Halsey, K. H., O'malley, R. T., Graff, J. R., Milligan, A. J., and Behrenfeld, M. J., A common partitioning strategy for photosynthetic products in evolutionarily distinct phytoplankton species, New Phytol., 198, 1030–1038, http://doi.org/10.1111/nph.12209, 2013.

Herman, P. M. J., Middelburg, J. J., van de Koppel, J., and Heip, C. H. R.: Ecology of estuarine macrobenthos, Adv. Ecol. Res., 29, 195–240, http://doi.org/10.1016/S0065-2504(08)60194-4, 1999.

25 Hickey, B. M., and Banas, N. S.: Oceanography of the U.S. Pacific Northwest coastal ocean and estuaries with application to coastal ecology, Estuaries, 26, 1010–1031, http://doi.org/10.1007/BF02803360, 2003.

Hily, C.: Is the activity of benthic suspension feeders a factor controlling water quality in the Bay of Brest? Mar. Ecol. Prog. Ser., 69, 179–188, http://doi.org/10.3354/meps069179, 1991.

Howarth, R. W., Swaney, D. P., Butler, T. J., and Marino, R.: Climatic control on eutrophication of the Hudson River
30 Estuary, Ecosystems, 3, 210–215, http://doi.org/10.1007/s100210000020, 2000.

Irby, I. D., Friedrichs, M. A., Da, F., and Hinson, K. E.: The competing impacts of climate change and nutrient reductions on dissolved oxygen in Chesapeake Bay, Biogeosciences, 15, 2649–2668, https://doi.org/10.5194/bg-15-2649-2018, 2018.

Jiang, L., Gerkema, T., Idier, D., Slangen, A. B. A., and Soetaert, K. E.: Effects of sea-level rise on tides and sediment dynamics in a Dutch tidal bay, Ocean Sci., 16, 307–321, https://doi.org/10.5194/os-16-307-2020, 2020.

Jiang, L., Gerkema, T., Wijsman, J. W., and Soetaert, K.: Comparing physical and biological impacts on seston renewal in a tidal bay with extensive shellfish culture, J. Mar. Syst., 194, 102–110, http://doi.org/10.1016/j.jmarsys.2019.03.003, 2019a.

Jiang, L., Soetaert, K., and Gerkema, T.: Decomposing the intra-annual variability of flushing characteristics in a tidal bay along the North Sea, J. Sea Res., 101821, https://doi.org/10.1016/j.seares.2019.101821, 2019b.

5   Jiang, L., and Xia, M.: Wind effects on the spring phytoplankton dynamics in the middle reach of the Chesapeake Bay, Ecol. Model., 363, 68–80, http://doi.org/10.1016/j.ecolmodel.2017.08.026, 2017.

Jiang, L., and Xia, M.: Modeling investigation of the nutrient and phytoplankton variability in the Chesapeake Bay outflow plume, Prog. Oceanogr., 162, 290–302, http://doi.org/10.1016/j.pocean.2018.03.004, 2018.

Jiang, L., Xia, M., Ludsin, S. A., Rutherford, E. S., Mason, D. M., Jarrin, J. M., and Pangle, K. L.: Biophysical modeling

10   assessment of the drivers for plankton dynamics in dreissenid-colonized western Lake Erie, Ecol. Model., 308, 18–33, http://doi.org/10.1016/j.ecolmodel.2015.04.004, 2015.

Kaufman, D. E., Friedrichs, M. A., Hemmings, J. C., and Smith Jr, W. O.: Assimilating bio-optical glider data during a phytoplankton bloom in the southern Ross Sea. Biogeosciences, 15, 73–90, https://doi.org/10.5194/bg-15-73-2018, 2018.

Kimmerer, W. J., and Thompson, J. K.: Phytoplankton growth balanced by clam and zooplankton grazing and net transport

15   into the low-salinity zone of the San Francisco Estuary, Estuaries Coast., 37, 1202–1218, http://doi.org/10.1007/s12237-013-9753-6, 2014.

Kromkamp, J., and Peene, J.: Possibility of net phytoplankton primary production in the turbid Schelde Estuary (SW Netherlands), Mar. Ecol. Prog. Ser., 121, 249–259, http://doi.org/10.3354/meps121249, 1995.

Kromkamp, J., Peene, J., van Rijswijk, P., Sandee, A., and Goosen, N.: Nutrients, light and primary production by

20   phytoplankton and microphytobenthos in the eutrophic, turbid Westerschelde estuary (The Netherlands), Hydrobiologia, 311, 9–19, http://doi.org/10.1007/BF00008567, 1995.

Kromkamp, J. C., and van Engeland, T.: Changes in phytoplankton biomass in the Western Scheldt Estuary during the period 1978–2006, Estuaries Coast., 33, 270–285, http://doi.org/10.1007/s12237-009-9215-3, 2010.

Lancelot, C., and Muylaert, K.: Trends in estuarine phytoplankton ecology. In *Treatise on estuarine and coastal science*,

25   Academic Press Waltham, 2011.

Lucas, L. V., Cloern, J. E., Thompson, J. K., Stacey, M. T., and Koseff, J. R.: Bivalve grazing can shape phytoplankton communities, Front. Mar. Sci., 3, 14, http://doi.org/10.3389/fmars.2016.00014, 2016.

Martin, M. A., Fram, J. P., and Stacey, M. T.: Seasonal chlorophyll a fluxes between the coastal Pacific Ocean and San Francisco Bay, Mar. Ecol. Prog. Ser., 337, 51–61, http://doi.org/10.3354/meps337051, 2007.

30   Miller, W., and Harding, L.W.: Climate forcing of the spring bloom in Chesapeake Bay, Mar. Ecol. Prog. Ser. 331, 11–22, http://doi.org/10.3354/meps331011, 2007.

Monbet, Y.: Control of phytoplankton biomass in estuaries: a comparative analysis of microtidal and macrotidal estuaries, Estuaries, 15, 563–571, http://doi.org/10.2307/1352398, 1992.

Muylaert, K., Tackx, M., and Vyverman, W.: Phytoplankton growth rates in the freshwater tidal reaches of the Schelde estuary (Belgium) estimated using a simple light-limited primary production model, Hydrobiologia, 540, 127–140, http://doi.org/10.1007/s10750-004-7128-5, 2005.

Nechad, B., Ruddick, K., and Park, Y.: Calibration and validation of a generic multisensor algorithm for mapping of total suspended matter in turbid waters, Remote Sens. Environ., 114, 854–866, http://doi.org/10.1016/j.rse.2009.11.022, 2010.

Nienhuis, P. H., and Smaal, A. C.: The Oosterschelde estuary, a case-study of a changing ecosystem: an introduction, Hydrobiologia, 282/283, 1–14, http://doi.org/10.1007/BF00024616, 1994.

North, E. W., Chao, S. Y., Sanford, L. P., and Hood, R. R.: The influence of wind and river pulses on an estuarine turbidity maximum: Numerical studies and field observations in Chesapeake Bay, Estuaries, 27, 132–146, http://doi.org/10.1007/BF02803567. 2004.

O'Donohue, M. J., and Dennison, W. C.: Phytoplankton productivity response to nutrient concentrations, light availability and temperature along an Australian estuarine gradient, Estuaries, 20, 521–533, http://doi.org/10.2307/1352611, 1997.

Qin, Q., and Shen, J.: The contribution of local and transport processes to phytoplankton biomass variability over different timescales in the Upper James River, Virginia. Estuar. Coast. Shelf Sci., 196, 123–133, https://doi.org/10.1016/j.ecss.2017.06.037, 2017.

Roegner, G. C., Hickey, B. M., Newton, J. A., Shanks, A. L., and Armstrong, D. A.: Wind-induced plume and bloom intrusions into Willapa Bay, Washington, Limnol. Oceanogr., 47, 1033–1042, http://doi.org/10.4319/lo.2002.47.4.1033, 2002.

Shen, J., Qin, Q., Wang, Y., and Sisson, M.: A data-driven modeling approach for simulating algal blooms in the tidal freshwater of James River in response to riverine nutrient loading, Ecological Modelling, 398, 44–54, https://doi.org/10.1016/j.ecolmodel.2019.02.005, 2019.

Sin, Y., Wetzel, R. L., and Anderson, I. C.: Spatial and temporal characteristics of nutrient and phytoplankton dynamics in the York River estuary, Virginia: Analyses of long-term data, Estuaries, 22, 260–275, http://doi.org/10.2307/1352982, 1999.

Smaal, A. C., Kater, B. J., and Wijsman, J. W. M.: Introduction, establishment and expansion of the Pacific oyster *Crassostrea gigas* in the Oosterschelde (SW Netherlands), Helgol. Mar. Res. 63, 75, doi 10.1007/s10152-008-0138-3, 2009.

Smaal, A. C., Schellekens, T., van Stralen, M. R., and Kromkamp, J. C.: Decrease of the carrying capacity of the Oosterschelde estuary (SW Delta, NL) for bivalve filter feeders due to overgrazing? Aquaculture, 404, 28–34, http://doi.org/10.1016/j.aquaculture.2013.04.008, 2013.

Soetaert, K., Herman, P. M., and Kromkamp, J.: Living in the twilight: estimating net phytoplankton growth in the Westerschelde estuary (The Netherlands) by means of an ecosystem model (MOSES), J. Plankton Res., 16, 1277–1301, http://doi.org/10.1093/plankt/16.10.1277, 1994.

Soetaert, K., Herman, P. M., Middelburg, J. J., Heip, C., Smith, C. L., Tett, P., and Wild-Allen, K.: Numerical modelling of the shelf break ecosystem: reproducing benthic and pelagic measurements, Deep-Sea Res. Pt. II, 48, 3141–3177, http://doi.org/10.1016/S0967-0645(01)00035-2, 2001.

17

Soetaert, K., Middelburg, J. J., Heip, C., Meire, P., Van Damme, S., and Maris, T.: Long-term change in dissolved inorganic nutrients in the heterotrophic Scheldt estuary (Belgium, The Netherlands), Limnol. Oceanogr., 51, 409–423, http://doi.org/10.4319/lo.2006.51.1_part_2.0409, 2006.

Son, S., Wang, M., and Harding, L.W.: Satellite-measured net primary production in the Chesapeake Bay, Remote Sens.
5 Environ. 144, 109–119, http://doi.org/10.1016/j.rse.2014.01.018, 2014.

Srichandan, S., Kim, J. Y., Kumar, A., Mishra, D. R., Bhadury, P., Muduli, P. R., Pattnaik, A. K., and Rastogi, G.: Interannual and cyclone-driven variability in phytoplankton communities of a tropical coastal lagoon, Mar. Pollut. Bull., 101(1), 39–52, http://doi.org/10.1016/j.marpolbul.2015.11.030, 2015.

Strayer, D. L., Pace, M. L., Caraco, N. F., Cole, J. J., and Findlay, S. E.: Hydrology and grazing jointly control a large-river
10 food web, Ecology, 89, 12–18, http://doi.org/10.1890/07-0979.1, 2008.

Tangelder, M., Troost, K., van den Ende, D., and Ysebaert, T.: Biodiversity in a changing Oosterschelde: from past to present, Wettelijke Onderzoekstaken Natuur & Milieu, WOT work document 288. pp. 52p, 2012.

Underwood, G. J. C. and Kromkamp J. C.: Primary production by phytoplankton and microphytobenthos in estuaries, Adv. Ecol. Res, 29, 93–153, http://doi.org/10.1016/S0065-2504(08)60192-0, 1999.

15 Valdes-Weaver, L. M., Piehler, M. F., Pinckney, J. L., Howe, K. E., Rossignol, K., and Paerl, H. W.: Long-term temporal and spatial trends in phytoplankton biomass and class-level taxonomic composition in the hydrologically variable Neuse-Pamlico estuarine continuum, North Carolina, U.S.A., Limnol. Oceanogr., 51, 1410–1420, http://doi.org/10.4319/lo.2006.51.3.1410, 2006.

van der Molen, J. S., and Perissinotto, R.: Microalgal productivity in an estuarine lake during a drought cycle: The St. Lucia
20 Estuary, South Africa, Estuar. Coast. Shelf Sci., 92, 1–9, http://doi.org/10.1016/j.ecss.2010.12.002, 2011.

van der Woerd, H. J., Blauw, A., Peperzak, L., Pasterkamp, R., and Peters, S.: Analysis of the spatial evolution of the 2003 algal bloom in the Voordelta (North Sea), J. Sea Res., 65, 195–204, http://doi.org/10.1016/j.seares.2010.09.007, 2011.

Vanhellemont, Q.: Adaptation of the dark spectrum fitting atmospheric correction for aquatic applications of the Landsat and Sentinel-2 archives, Remote Sens. Environ., 225, 175–192, http://doi.org/10.1016/j.rse.2019.03.010 2019.

25 Vanhellemont, Q., and Ruddick K.: Acolite for Sentinel-2: aquatic applications of MSI imagery. ESA Special Publication SP-740. ESA Living Planet Symposium, Prague, Czech Republic, 9–13 May 2016. http://odnature.naturalsciences.be/downloads/ publications/2016_Vanhellemont_ESALP.pdf, 2016.

Vanhellemont, Q., and Ruddick, K.: Atmospheric correction of metre-scale optical satellite data for inland and coastal water applications, Remote Sens. Environ., 216, 586–597, http://doi.org/10.1016/j.rse.2018.07.015, 2018.

30 Vroon, J.: Hydrodynamic characteristics of the Oosterschelde in recent decades, Hydrobiologia, 282/283, 17–27, http://doi.org/10.1007/BF00024618, 1994.

Wetsteyn, L. P. M. J., and Kromkamp, J. C.: Turbidity, nutrients and phytoplankton primary production in the Oosterschelde (The Netherlands) before, during and after a large-scale coastal engineering project (1980–1990), Hydrobiologia, 282/283, 61–78, http://doi.org/10.1007/BF00024622, 1994.

Wijsman, J. W. M., and Smaal, A. C.: The use of shellfish for pre-filtration of marine intake water in a reverse electro dialysis energy plant; Inventory of potential shellfish species and design of conceptual filtration system. Report C078/17, Wageningen Marine Research, the Netherlands, 2017.

Wijsman, J. W. M., Troost, K., Fang, J., and Roncarati, A.: Global production of marine bivalves: Trends and challenges, In Goods and Services of Marine Bivalves, edited by Smaal et al., Springer, Cham, Switzerland, http://doi.org/10.1007/978-3-319-96776-9_2, 2019.

Ysebaert, T., van der Hoek, D. J., Wortelboer, R., Wijsman, J. W., Tangelder, M., and Nolte, A.: Management options for restoring estuarine dynamics and implications for ecosystems: A quantitative approach for the Southwest Delta in the Netherlands, Ocean Coast. Manage., 121, 33–48, http://doi.org/10.1016/j.ocecoaman.2015.11.005, 2016.

Table 1: Formulations in the biogeochemical model in this study. Parameters and variables in each equation are described in Table 2.

$$T_{fac} = Q_{10}^{(T-T_{ref})/T}$$	(1)
$$\text{DinUpt} = \text{maxUpt} \cdot T_{fac} \cdot \frac{DIN}{DIN + ksDIN} \cdot \frac{PAR}{PAR + ksPAR} \cdot PHY$$	(2)
$$\text{ZooGrz} = \text{maxGrzZoo} \cdot T_{fac} \cdot \frac{PHY}{PHY + ksGrzZoo} \cdot ZOO$$	(3)
$$\text{ZooGro} = (1 - \text{pFaeZoo}) \cdot \text{ZooGrz}$$	(4)
$$\text{ZooExc} = \text{excRZoo} \cdot T_{fac} \cdot ZOO$$	(5)
$$\text{ZooMor} = \text{morRZoo} \cdot T_{fac} \cdot ZOO \cdot ZOO$$	(6)
$$\text{Min} = \text{minR} \cdot T_{fac} \cdot DET$$	(7)
$$\text{BotMin} = \text{minR} \cdot T_{fac} \cdot BDET$$	(8)
$$\text{SinDet} = \text{sinRDet} \cdot DET$$	(9)
$$\text{SinPhy} = \text{sinRPhy} \cdot PHY$$	(10)
$$BivGrz_{i=1,2,3} = maxClr_i \cdot T_{fac} \cdot BIV_i \cdot (PHY + ZOO + DET)$$	(11)
$$BivGro_{i=1,2,3} = (1 - pRspBiv_i) \cdot (1 - pFaeBiv_i - pPsfBiv_i) \cdot BivGrz_i$$	(12)
$$BivExc_{i=1,2,3} = excRBiv_i \cdot T_{fac} \cdot BIV_i$$	(13)
$$\text{MpbDinUpt} = \text{maxUptMpb} \cdot T_{fac} \cdot \frac{DIN}{DIN + ksDINMpb} \cdot \frac{PAR}{PAR + ksPARMpb} \cdot MPB$$	(14)
$$\text{MpbMor} = \text{morRMpb} \cdot T_{fac} \cdot MPB \cdot MPB$$	(15)
$$dDIN/dt = Min + ZooExc - DinUpt + [(1 - pLos)BotMin + BivExc + \sum_{i=1,2,3} pRspBiv_i BivFrz_i - DinUptMpb]/z$$	(16)
$$dPHY/dt = DinUpt - ZooGrz - (SinPhy + \sum_{i=1,2,3} maxClr \cdot T_{fac} \cdot BIV_i \cdot PHY)/z$$	(17)
$$dZOO/dt = ZooGro - ZooExc - ZooMor - \sum_{i=1,2,3} maxClr \cdot T_{fac} \cdot BIV_i \cdot ZOO /z$$	(18)
$$dDET/dt = ZooMor + \text{pFaeZoo} \cdot ZooGrz - Min - (SinDet + \sum_{i=1,2,3} maxClr \cdot T_{fac} \cdot BIV_i \cdot DET)/z$$	(19)
$$dBDET/dt = SinDet + SinPhy - BotMin + \sum_{i=1,2,3} (pFaeBiv_i + pPsfBiv_i) \cdot BivGrz_i + MpbMor$$	(20)
$$dBIV/dt = BivGro - BivExc$$	(21)
$$dMPB/dt = \text{MpbDinUpt} - MpbMor$$	(22)

5

10

Table 2: Main variables (bold) and parameters (underlined, followed by values) in equations in Table 1. The parameter values are based on ranges in prior literature (Soetaert et al., 2001; Jiang ~~et al.~~ and Xia, 2017; Wijsman and Smaal, 2017) and tuned for our application.

|	
T_{fac}, temperature factor, dimensionless; T, *in situ* temperature, °C; T_{ref} = 10 °C, reference temperature; Q_{10} = 2, temperature coefficient	(1)
DIN, state variable, dissolved inorganic nitrogen, mmol m^{-3}; PHY, state variable, phytoplankton biomass, mmol m^{-3}; $DinUpt$, pelagic DIN uptake, mmol m^{-3} d^{-1}; PAR, *in situ* photosynthetically active radiation, µmol-photons m^{-2} s^{-1}; $maxUpt$ = 1.7 d^{-1}, maximum DIN uptake rate; $ksDIN$ = 1 mmol m^{-3}, half-saturation DIN concentration; $ksPAR$ = 140 µmol-photons m^{-2} s^{-1}, half-saturation PAR	(2)
ZOO, state variable, zooplankton biomass, mmol m^{-3}; $ZooGrz$, zooplankton grazing, mmol m^{-3} d^{-1}; $maxGrzZoo$ = 0.8 d^{-1}, maximum zooplankton grazing rate; $ksGrzZoo$ = 0.6 mmol m^{-3}, half-saturation phytoplankton concentration for zooplankton grazing	(3)
$ZooGro$, zooplankton growth, mmol m^{-3} d^{-1}; $pFecZoo$ = 0.3, fraction of zooplankton faeces in total grazing	(4)
$ZooExc$, zooplankton excretion, mmol m^{-3} d^{-1}; $excRZoo$ = 0.08 d^{-1}, zooplankton excretion rate	(5)
$ZooMor$, zooplankton mortality, mmol m^{-3} d^{-1}; $morRZoo$ = 0.45 m^3 mmol^{-1} d^{-1}, quadratic zooplankton mortality rate	(6)
DET, state variable, pelagic detritus, mmol m^{-3}; Min, DIN regeneration from pelagic detritus, mmol m^{-3} d^{-1}; $minR$ = 0.02 d^{-1}, mineralization rate	(7)
$BDET$, state variable, benthic detritus, mmol m^{-2}; $BotMin$, DIN regeneration from benthic detritus, mmol m^{-2} d^{-1}	(8)
$SinDet$, detritus sinking, mmol m^{-2} d^{-1}; $sinRDet$ = 1.0 m d^{-1}, sinking rate of detritus	(9)
$SinPhy$, phytoplankton sinking, mmol m^{-2} d^{-1}; $sinRPhy$ = 0.2 m d^{-1}, sinking rate of phytoplankton	(10)
$BIV_{1,2,3}$, state variable, biomass of bivalve filter feeding mussels, oysters, and cockles (1–3 denotes these three species hereafter), mmol m^{-2}, $BivGrz_{1,2,3}$, bivalve grazing rate, mmol m^{-2} d^{-1}; $maxClr_{1,2,3}$ = 0.007, 0.015, 0.0037 m^3 mmol^{-1} d^{-1}	(11)
$BivGro_{1,2,3}$, bivalve growth, mmol m^{-2} d^{-1}; $pRspBiv_{1,2,3}$ = 0.001, 0.003, 0.001, bivalve respiration portion in the net assimilation; $pFecBiv_{1,2,3} + pPsfBiv_{1,2,3}$ = 0.55, 0.39, 0.33, fraction of bivalve faeces (*Fec*) and pseudo-faeces (*Psf*) in total grazing	(12)
$BivExc_{1,2,3}$, bivalve excretion, mmol m^{-2} d^{-1}; $excRBiv_{1,2,3}$ = 0.0006, 0.0001, 0.001 d^{-1}, bivalve excretion rates	(13)
MPB, state variable, microphytobenthos biomass, mmol m^{-2}; $DinUptMpb$, microphytobenthic DIN uptake, mmol m^{-2} d^{-1}; $maxUpt$ = 0.75 d^{-1}, maximum microphytobenthic DIN uptake rate; $ksDINMpb$ = 1 mmol m^{-3}, half-saturation DIN concentration for microphytobenthos; $ksPARMpb$ = 100 µmol-photons m^{-2} s^{-1}, half-saturation PAR for microphytobenthos	(14)
$MpbMor$, microphytobenthos mortality, mmol m^{-2} d^{-1}; $morRMpb$ = 0.001 m^2 mmol^{-1} d^{-1}, quadratic microphytobenthos mortality rate	(15)
$dDIN/dt$, $dPHY/dt$, $dZOO/dt$, $dDET/dt$, change rates of pelagic variables, mmol m^{-3} d^{-1}; $dBDET/dt$, $dBIV/dt$, $dMPB/dt$, change rates of benthic variables, mmol m^{-2} d^{-1}; z, thickness of the bottom layer, m	(16–22)
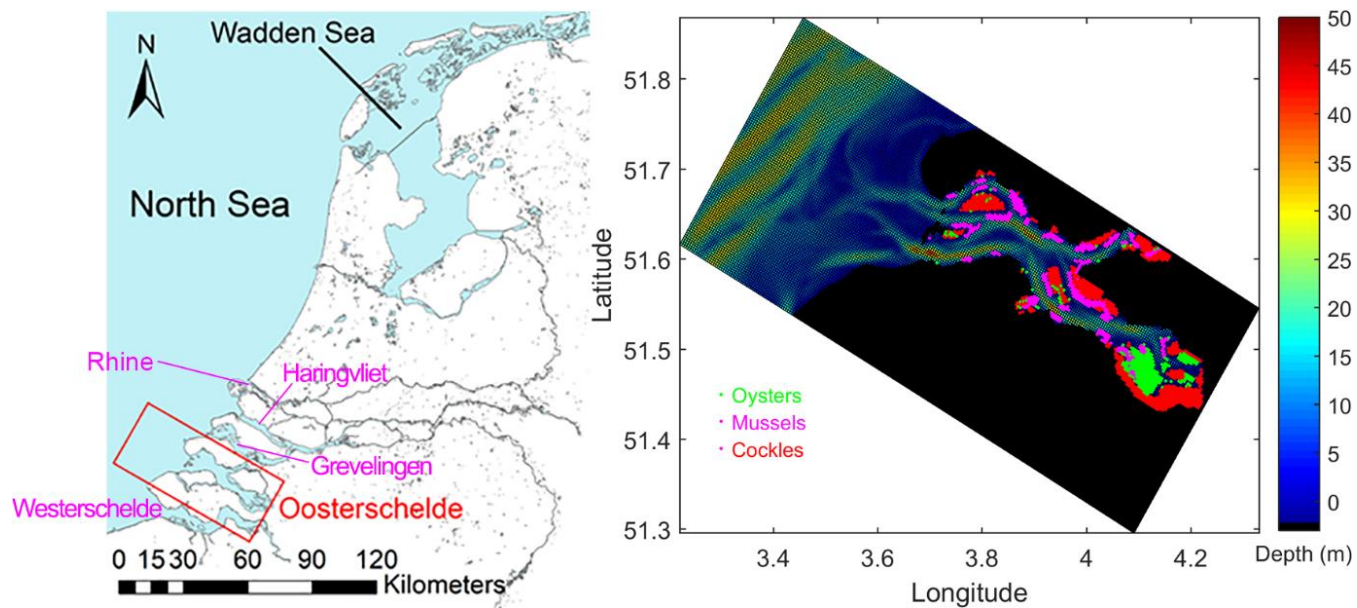
Figure 1: Geographic location of the Oosterschelde and the GETM-FABM model grid, domain, and bathymetry. Green, pink, and red dots in the right panel indicate the distribution of three dominant bivalve species in the Oosterschelde, oysters, mussels, and cockles (data source: Wageningen Marine Research).
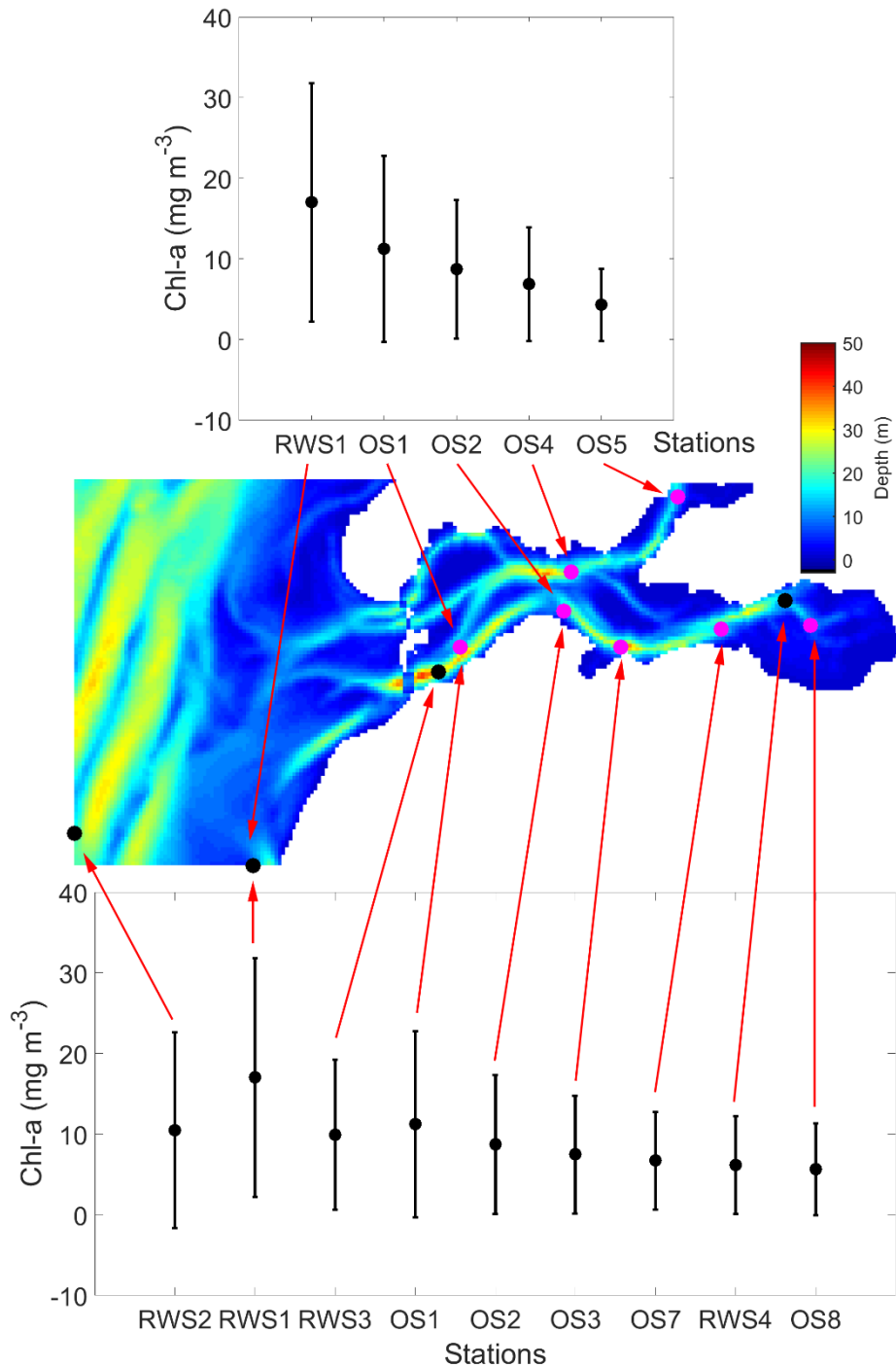
Figure 2: Average spring (March to May) chlorophyll a (chl-a) concentration during 1995–2013 at NIOZ (OS1–OS8) and Rijkswaterstaat (RWS1–RWS4) monitoring stations. The error bars of each stations indicate standard deviations. The map shows bathymetry in the GETM-FABM model domain denoted in Figure 1 and marks all NIOZ and RWS stations within the domain. RWS1–RWS4 in this study are short names for Walcheren 2 km, Walcheren 20 km, Wissenkerke, and Lodijkse Gat in the RWS database, respectively.
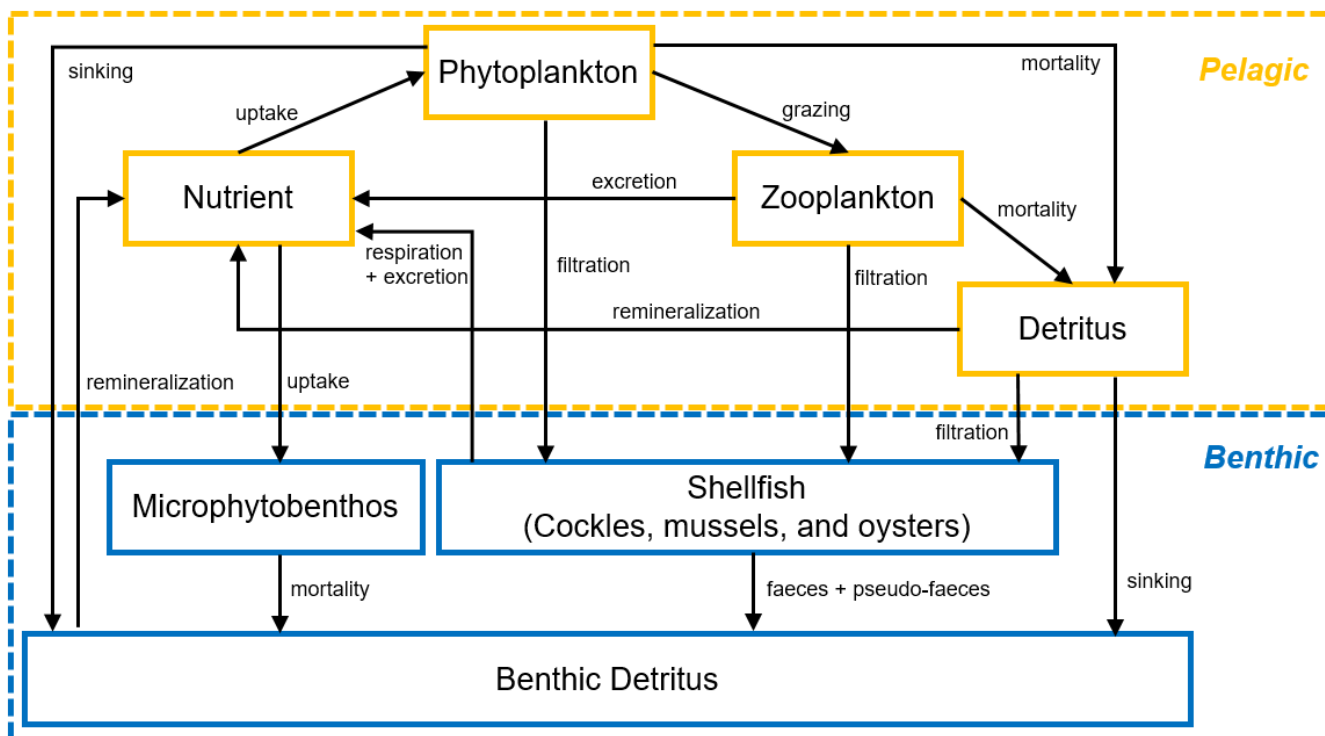
Figure 3: Conceptual diagram of the nitrogen-based seven-variable biogeochemical model structure in FABM. Box and arrows denote state variables and fluxes of nitrogen, respectively.
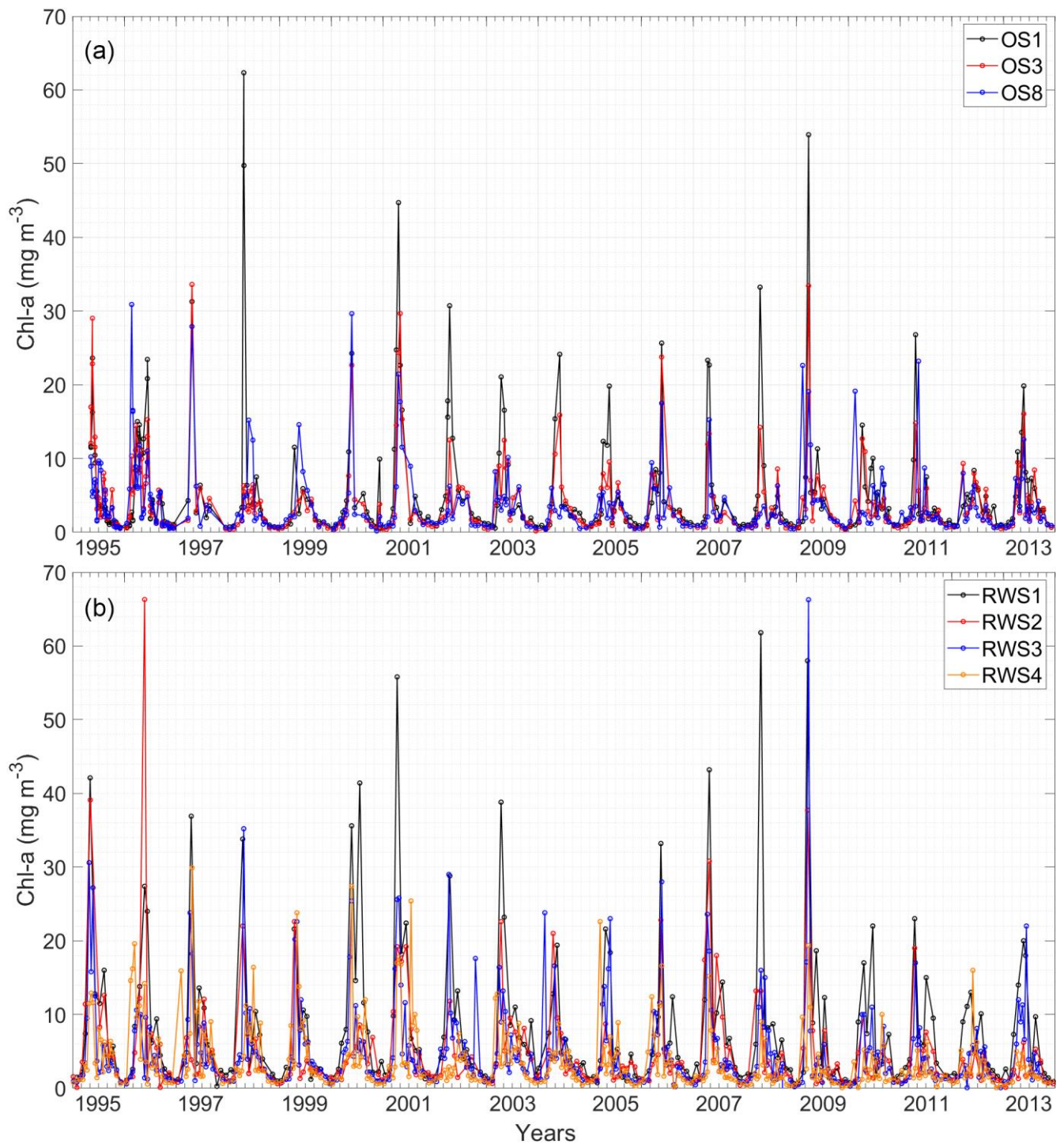
Figure 4: Time series of chlorophyll a (chl-a) concentrations during 1995–2013 at (a) NIOZ stations OS1, OS3, and OS8 and (b) Rijkswaterstaat stations RWS1–RWS4. Intervals between grid lines indicate two months. See Figure 2 for station locations.
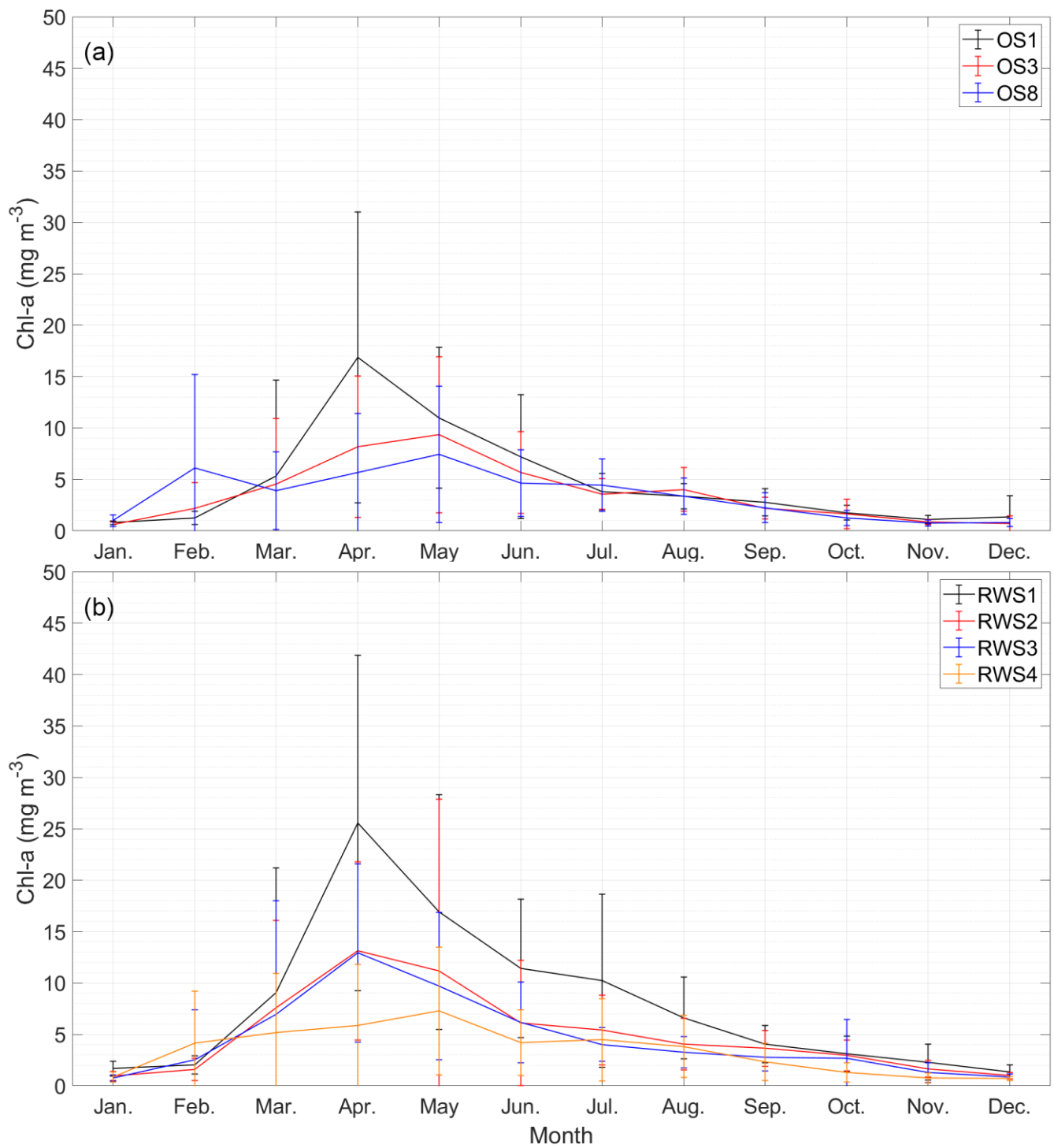
Figure 5: Monthly average chlorophyll a (chl-a) concentrations during 1995–2013 at (a) NIOZ stations OS1, OS3, and OS8 and (b) Rijkswaterstaat stations RWS1–RWS4. The error bars of each station indicate standard deviations. See Figure 2 for station locations.
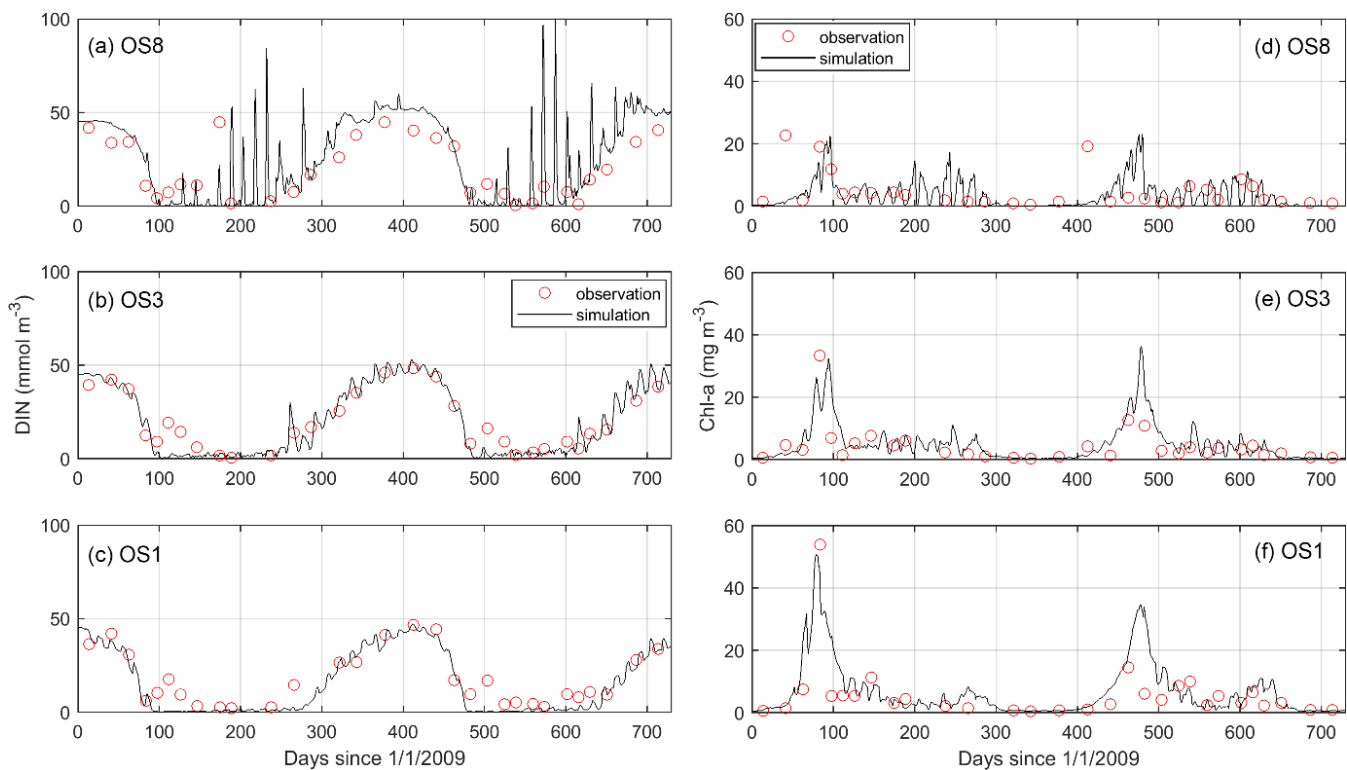
Figure 6: Comparison between simulated and observed dissolved inorganic nitrogen (DIN) and chlorophyll a (chl-a) in the years 2009–2010 at stations OS8, OS3, and OS1. See Figure 2 for station locations.
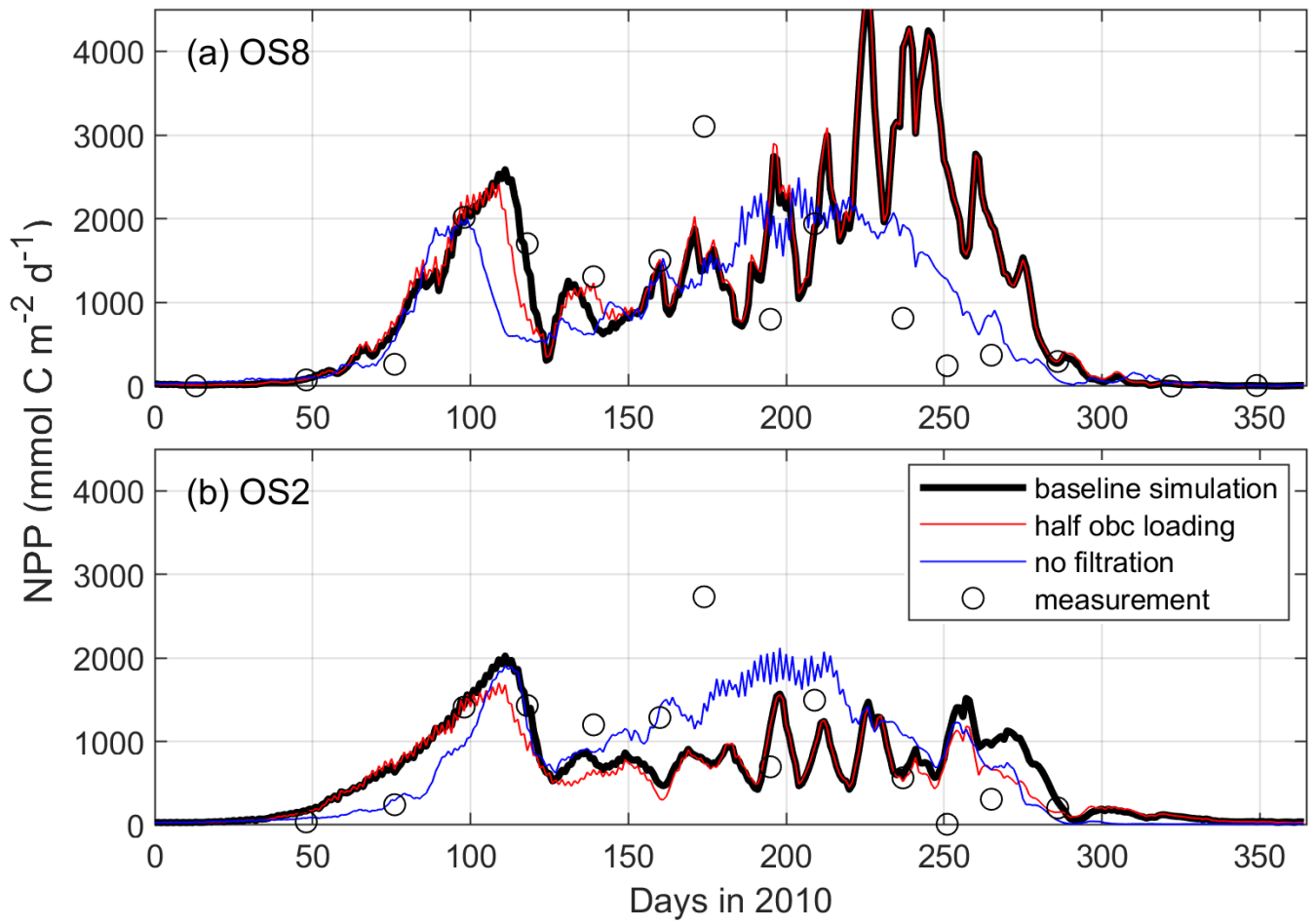
Figure 7: Comparison between modeled and measured depth-integrated net primary production (NPP, mmol carbon m^{-2} d^{-1}) in 2010 at stations OS8 and OS2. The three model scenarios include the baseline scenario, halving the open boundary nutrient and phytoplankton loading, and switching off bivalve filtration feeders.
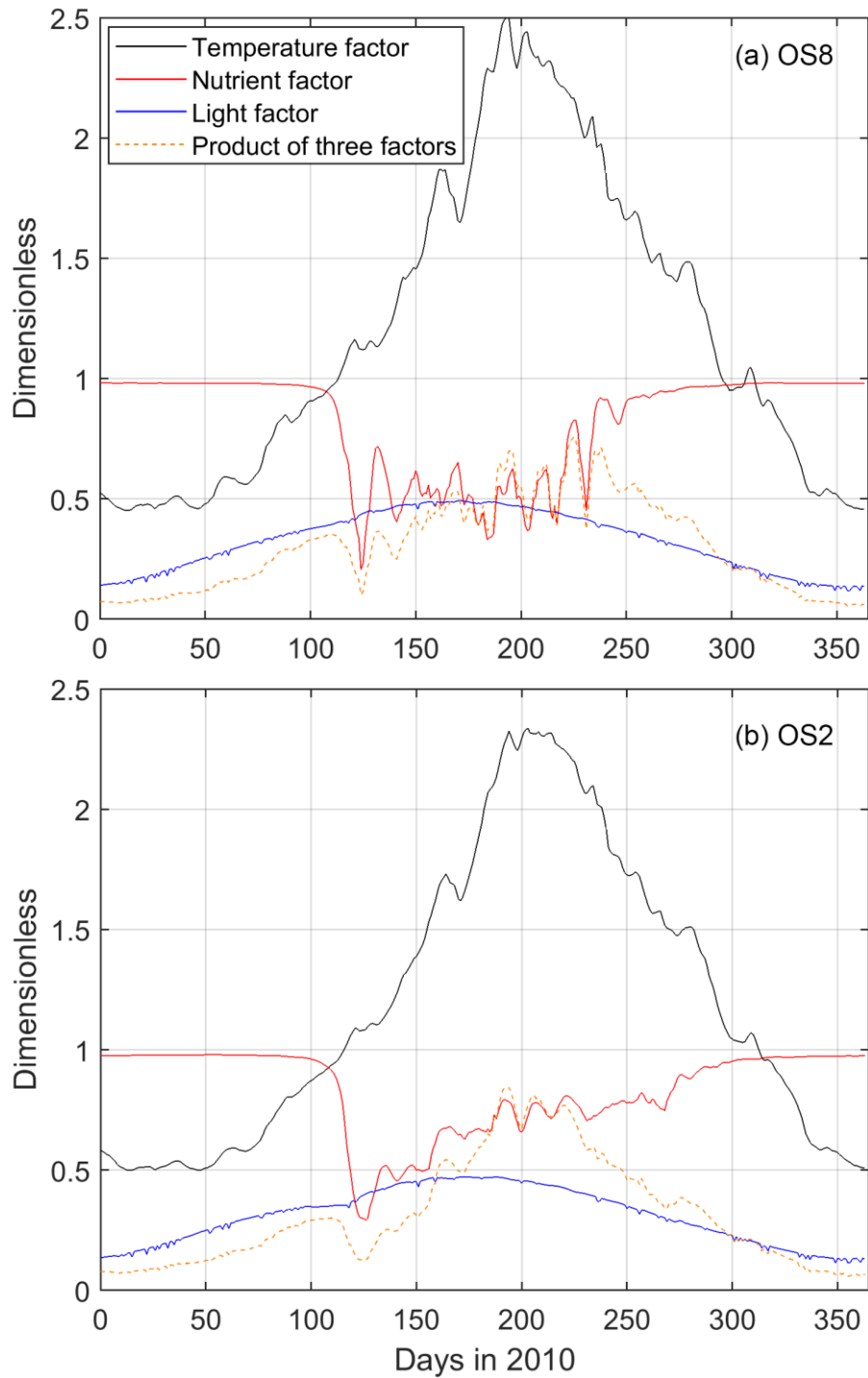
Figure 8: Modeled surface temperature, nutrient, and light factors affecting the phytoplankton growth rate at (a) OS 8 and (b) OS2. Temperature factor is calculated as Equation (1) in Table 1. Nutrient factor = *DIN* / (*DIN* + *ksDIN*), light factor = *PAR* / (*PAR* + *ksPAR*), as shown in Equation (2) in Table 1. According to Equation (2), the product of these three factors is positively related to phytoplankton growth rate.
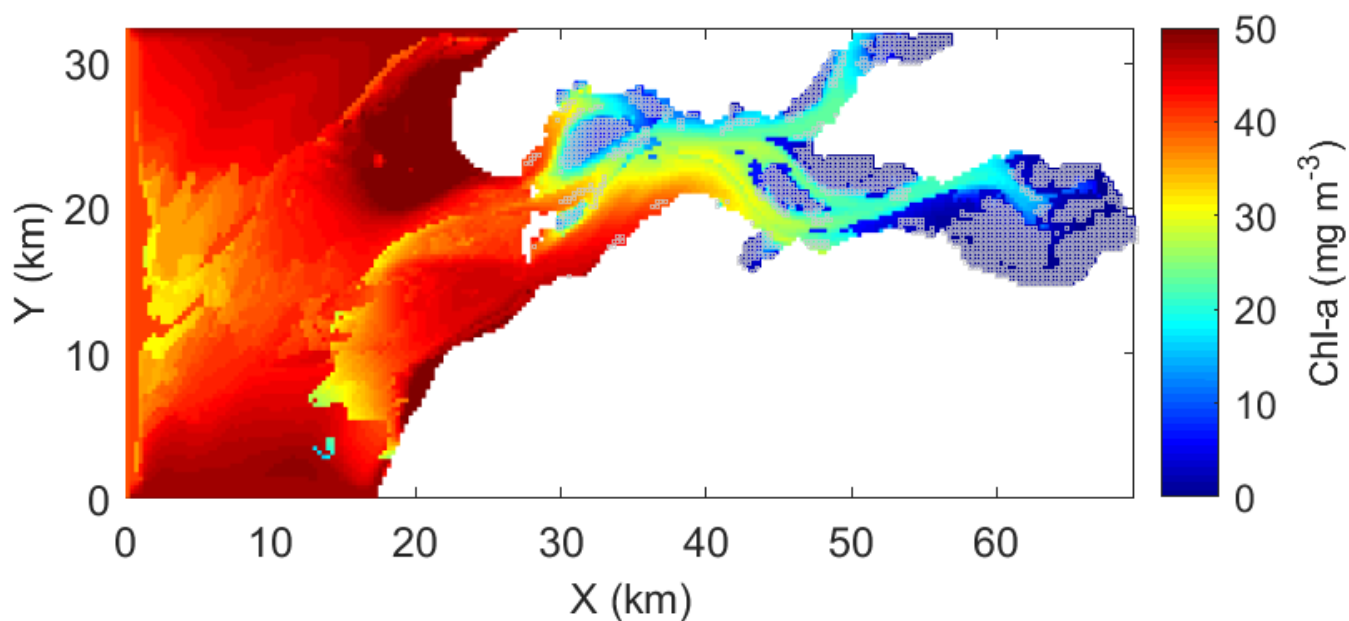
Figure 89: The 15-day (5–19 March) average of modeled chlorophyll a (chl-a) during the peak spring bloom in 2009. Grey squares indicate the locations of wild and cultured shellfish as in Figure 1.
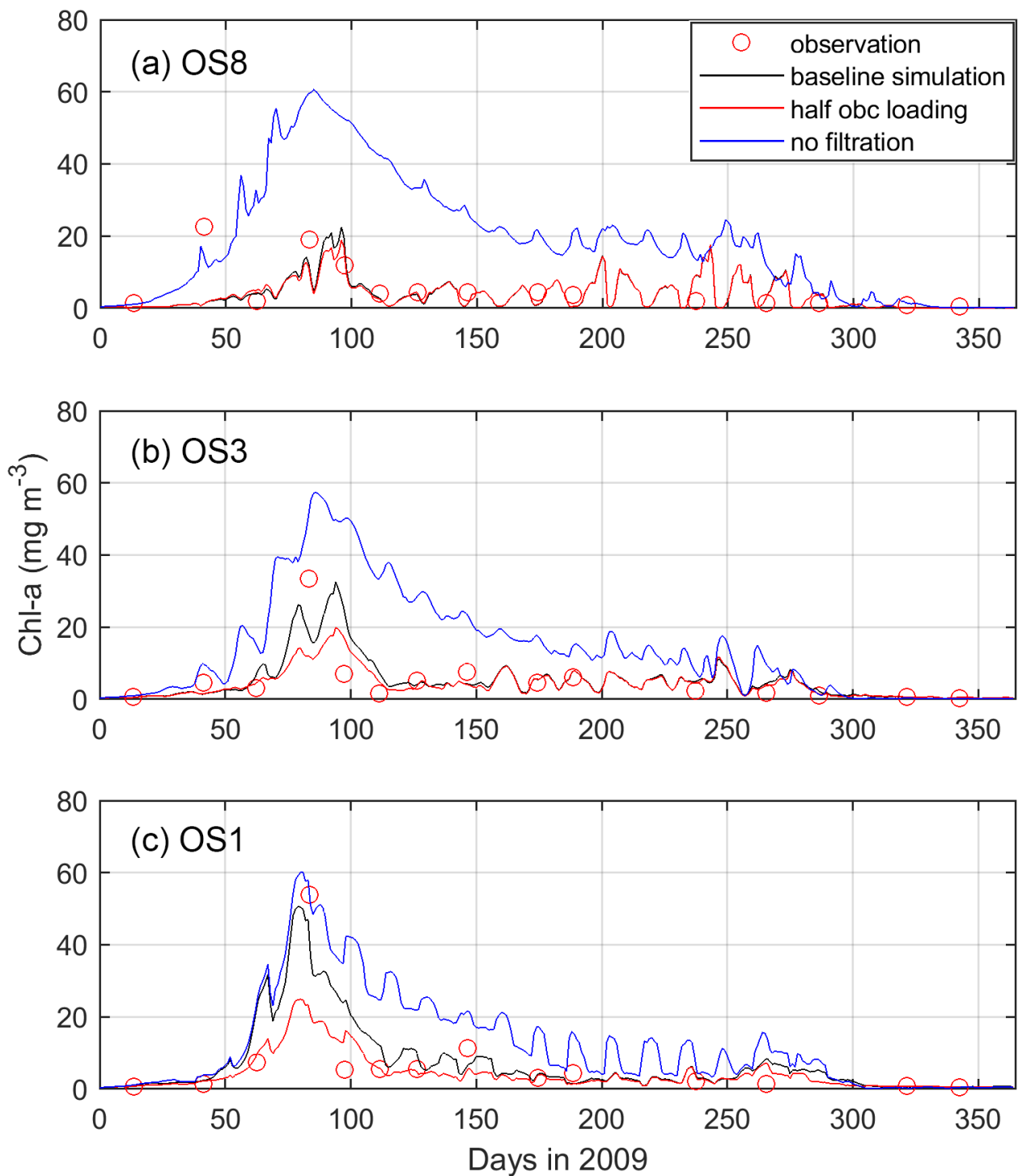
Figure 910: Modeled and observed chlorophyll a (chl-a) in 2009 at stations OS8, OS3, and OS1. The three model scenarios include the baseline scenario, halving the open boundary nutrient and phytoplankton loading, and switching off bivalve filtration feeders. See Figure 2 for station locations.
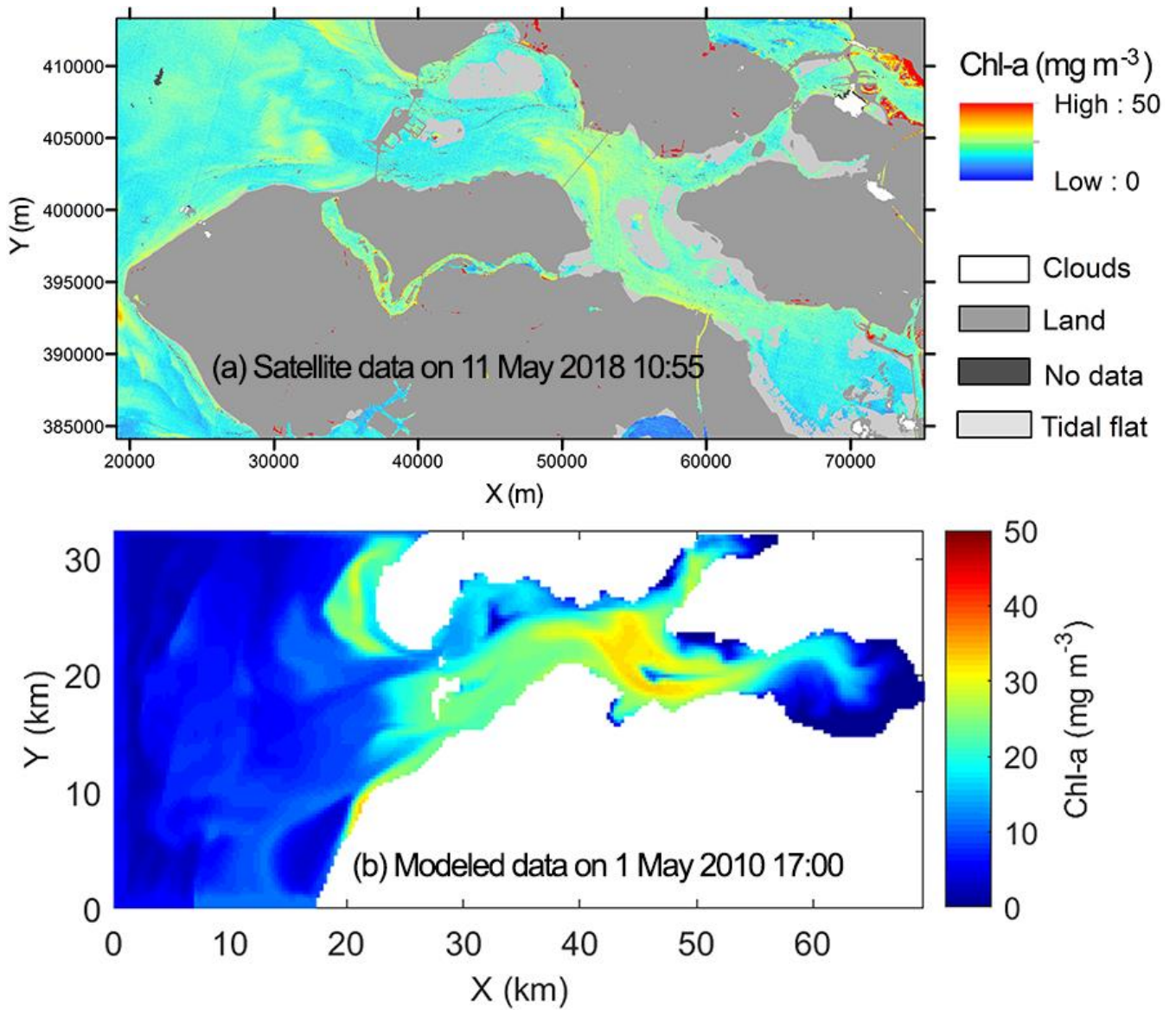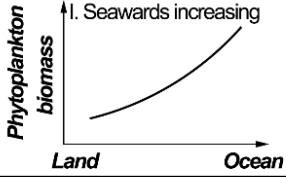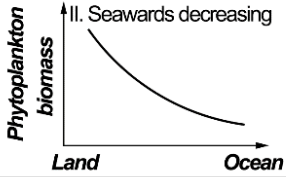
Figure 101. Chlorophyll a (chl-a) in the Oosterschelde retrieved from (a) a high tide Sentinel-2 MSI image of 11 May 2018, at 10:55 masking tidal flats from a low tide Sentinel-2 MSI image of 21 April 2019 and (b) the model on 1 May 2010, at 17:00. Both snapshots are during high tide. The coordinate system in (a) is EPSG:28992, Amersfoort / RD New.
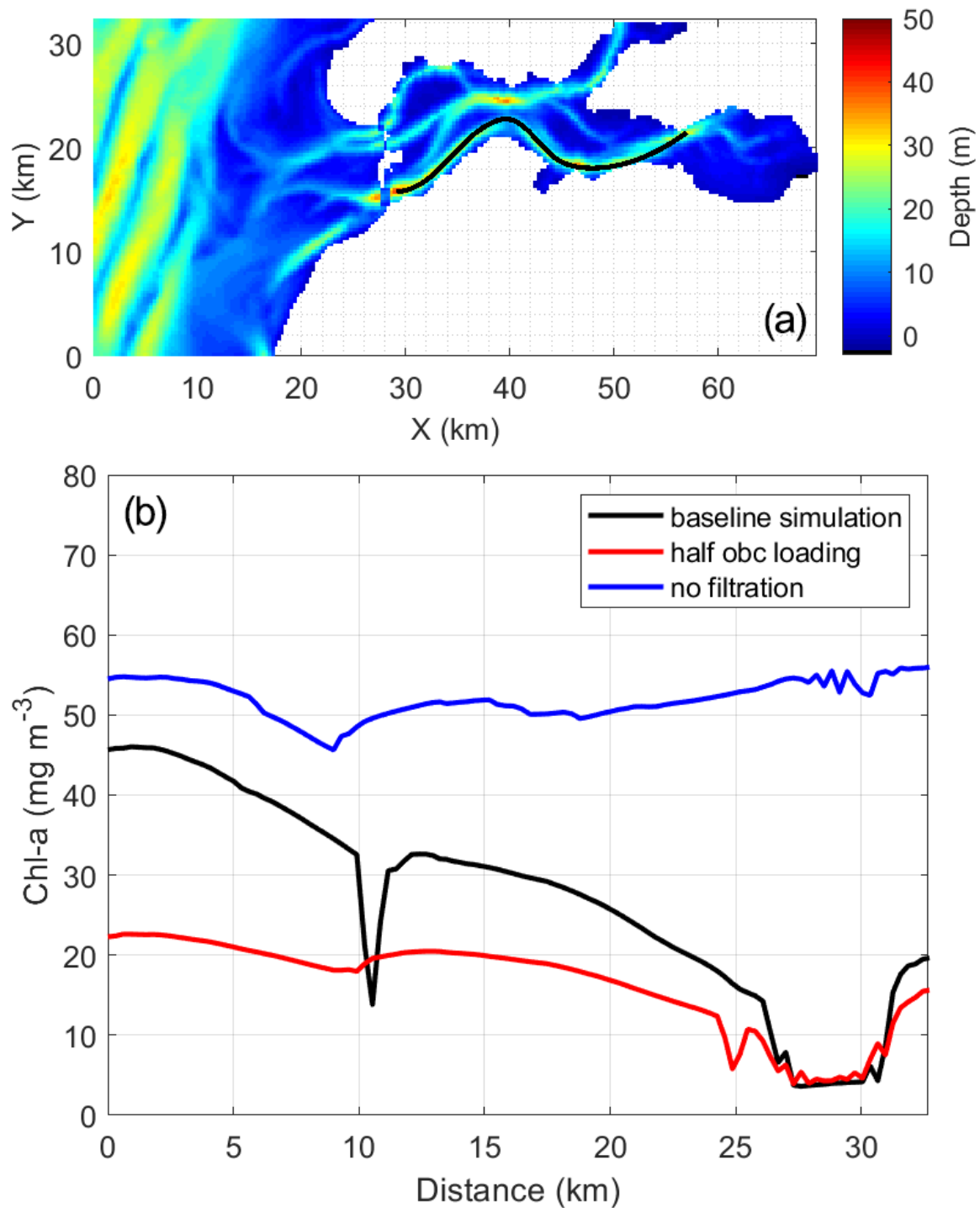
Figure 1~~1~~2. (b) The 15-day (5–19 March) average of modeled chlorophyll a (chl-a) during the peak spring bloom in 2009 along (a) a transect over the southern channel of the Oosterschelde. The distance on the x-axis of panel (b) is from west to east. The three model scenarios include the baseline scenario, halving the open boundary nutrient and phytoplankton loading, and switching off bivalve filtration feeders.
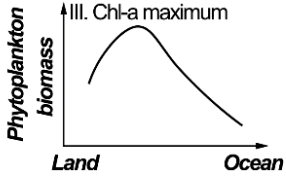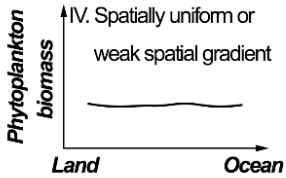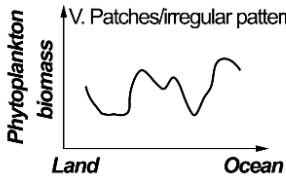
Types of spatial gradients	Example ecosystems and references	Flushing mechanisms	Main drivers of phytoplankton biomass
I. Seawards increasing (Phytoplankton biomass vs Land–Ocean)	(1) Oosterschelde, the Netherlands (this study)	Tide-dominated	Grazing loss and tidal import
	(2) Rías Baixas of Galicia, Spain (Figueiras et al., 2002); Willapa Bay, USA (Hickey and Banas, 2003; Banas et al., 2007)	Tide-dominated	Tidal import
	(3) Chilika Lagoon, India (Srichandan et al., 2015)	River-dominated	Light limitation
II. Seawards decreasing (Phytoplankton biomass vs Land–Ocean)	(1) Westerschelde estuary, the Netherlands and Belgium (Kromkamp and Peene, 1995; Krompkamp et al., 1995; Muylaert et al., 2005; Soetaert et al., 1994, 2006)	River and tides, or river-dominated	Salinity stress, grazing loss, and transport
	(2) Chesapeake Bay outflow plume, USA (Jiang and Xia, 2018); Mississippi River plume, USA (Gomez et al., 2018)	River and tides	Nutrient limitation
III. Chl-a maximum (Phytoplankton biomass vs Land–Ocean)	(1) Chesapeake Bay, USA (Jiang and Xia, 2017); Delaware Bay, USA (Fisher et al., 1988); York River, USA (Sin et al., 1999); Neuse-Pamlico estuary, USA (Valdes-Weaver et al., 2006); Logan River and Moreton Bay, Ausatralia (O'Donohue and Dennison, 1997)	River and tides, or river-dominated	Upper reach limited by light or transport loss; lower reach limited by nutrients
IV. Spatially uniform or weak spatial gradient (Phytoplankton biomass vs Land–Ocean)	(1) San Francisco Bay, USA , after 1987 (Cloern et al., 2017; Kimmerer and Thompson, 2014)	River and tides	Grazing loss
	(2) Hudson River estuary, USA (Fisher et al., 1988; Howarth et al., 2000; Strayer et al., 2008)	River-dominated	Transport and grazing loss
V. Patches/irregular patterns (Phytoplankton biomass vs Land–Ocean)	(1) Baie des Veys estuary, France (Grangeré et al., 2010)	River and tides	Grazing loss
	(2) Krka estuary, Croatia (Ahel et al., 1996)	River-dominated	Point-source nutrient input
	(3) St. Lucia estuary, South Africa (van der Molen and Perissinotto, 2011)	River-dominated	DIN:DIP ratio, salinity, temperature, and irradiance

Figure 1~~2~~3. ~~A summary of various~~ Common spatial ~~gradients~~ patterns of phytoplankton biomass ~~reported in literature~~ in estuarine-coastal systems. For comparison with the Oosterschelde, ~~A few examples of~~ example ecosystems for each type are given along with references, the dominant flushing mechanisms, and main drivers of phytoplankton accumulation ~~in the specific ecosystems~~.

5

34